

Graph-based Facial Affect Analysis: A Review of Methods, Applications and Challenges

Yang Liu, Xingming Zhang, Jinzhao Zhou, Xin Li, Yante Li, and Guoying Zhao, *Senior Member, IEEE*

Abstract—Facial affect analysis (FAA) using visual signals is a key step in human-computer interactions. Early methods mainly focus on extracting appearance and geometry features associated with human affects, while ignore the latent semantic information among individual facial changes, leading to limited performance and generalization. Recent trends attempt to establish a graph-based representation to model these semantic relationships and develop learning frameworks to leverage it for different FAA tasks. In this paper, we provide a comprehensive review of graph-based FAA, including the evolution of algorithms and their applications. First, we introduce the background knowledge of facial affect analysis, especially on the role of graph. We then discuss approaches that are widely used for graph-based affective representation in literatures and show a trend towards graph construction. For the relational reasoning in graph-based FAA, we categorize the existing studies according to their usage of traditional methods or deep models, with a special emphasis on latest graph neural networks. Experimental comparisons of the state-of-the-art on standard FAA problems are also summarized. Finally, we discuss the challenges and potential directions. As far as we know, this is the first survey of graph-based FAA methods, and our findings can serve as a reference point for future research in this field.

Index Terms—Facial Affect Analysis, Facial Expression Recognition, Micro-expression Recognition, Action Unit Detection, Affective Graph Representation, Graph Neural Network.

1 INTRODUCTION

FACIAL affect is one of the greatest important visual signals for developing human-computer interaction (HCI) systems, because it conveys critical information that reflects emotional states and reactions in human communications [1], [2], [3]. During the past two decades, many facial affect analysis (FAA) methods have been explored based on interdisciplinary progresses of computer vision, cognitive neuroscience and psychology [4], [5], [6], and some of them have been extended to various applications including medical diagnosis [7], education [8] and virtual reality [9]. Despite the successes, there are still some challenging gaps, such as coarse-grained to fine-grained affect representation, constrained to in-the-wild affect prediction, and discrete affect recognition to continuous affect intensity estimation.

Before going into the field of FAA, we need first know what the facial affect is. As early as 1970s, Paul Ekman *et al.* [10] proposed the definition of six basic emotions, i.e., *happiness, sadness, fear, anger, disgust, and surprise*, based on an assumption of the universality of human affective display [11]. This definition has been followed for many years till now. Besides, another popular affect description model, called the Facial Action Coding System (FACS), was designed for a wider range of emotions, which consists of a set of atomic Action Units (AUs) [12], [13]. Figure 1 shows an example of six basic emotions plus *neutral* as well as

activated AUs in each facial affect. Both the two affective models are categorical one that depicts discrete human emotions. There are other findings suggesting a dimensional affective model [14], [15], [16], with valence and arousal (V-A), which is considered more appropriate to describe dynamic changes of human affects in real world.



Fig. 1. An example of basic facial affects and related AU marks. AU0 denotes no activated AU. Images are from BU-4DFE database [17]. From left to right: anger, disgust, fear and neutral (top); happiness, sadness and surprise (bottom).

- Y. Liu, X. Zhang, J. Zhou and X. Li are with the School of Computer Science and Engineering, South China University of Technology, Guangzhou 510006, China.
E-mail: liuy17@163.com, cszxm@scut.edu.cn, charlesmzhouscut@gmail.com, lixin_forget@163.com,
- Y. Liu, Y. Li and G. Zhao are with the Center for Machine Vision and Signal Analysis, University of Oulu, Oulu, FI-90014, Finland.
E-mail: {firstname.lastname}@oulu.fi

Manuscript received XX XX, 20XX; revised XX XX, 20XX.

In the community of computer vision and affective computing, several competitions (challenges) are held periodically to evaluate the latest progress of FAA and propose frontier research trends. The Facial Expression Recognition and Analysis (FERA) challenge (FG 2011, 2015, 2017) focuses on AU detection and emotion recognition [18], and gradually introduces more complex factors such as intensity

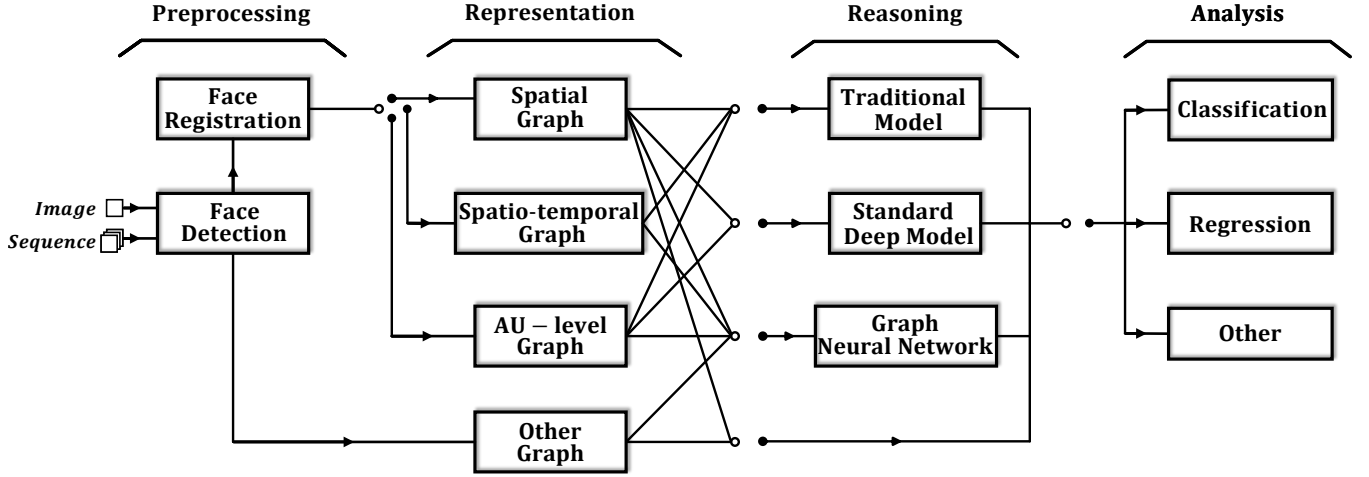


Fig. 2. The pipeline of graph-based facial affect analysis methods.

estimation and non-frontal head poses [19]. Moreover, the Emotion Recognition in the Wild (EmotiW) challenge (ICMI 2013-2020) [20], the Faces in-the-wild workshop-Challenge (Wild-Face) (CVPR 2017) [21] and the EmotioNet Challenge (ENC) (2017, 2018, CVPR 2020) [22] pay more attention on discrete or continuous (V-A) facial affects in real world scenarios. Besides, the Audio/Visual Emotion Challenge (AVEC) (ACII 2011, ACM MM 2012-2019) [23] and the Multimodal Sentiment in Real-life Media Challenge (MuSe) (ACM MM'2020) [24] aim at analyzing human sentiment in a multi-modality manner. These competitions also provide universal annotated data and standard benchmarks that promotes the development in FAA field.

Accordingly, FAA methods have experienced a series of historical evolution. Initial studies mostly rely on hand-crafted features or classic machine learning to obtain useful affective information [4]. With the wave of the deep learning, the performance of various FAA tasks has been promoted into a new high level without tedious feature design and selection. Nevertheless, these methods often only use raw images or simple facial partitions. They ignore key context and latent semantic information in facial affects [25], which limits effectiveness and capability. Thus, a good facial affective representation is crucial for optimizing the feature learning process. Recently, graph-based FAA has received increasing attention, not only because it has more consistent representation with facial muscle anatomical definition [26], but also it is easier to encode prior knowledge for advanced affective features by using the graph structure.

In this paper, we review the state of research on facial affect analysis using graph-based methods. Although there are many reviews that have discussed the historical evolution [4], [27], [28] and recent advances [29], [30], [31] of FAA, including some on specific problems like occlusion expression [32], micro-expression [33] and multi-modal affect [34], this is the first systematic and in-depth survey of the graph-based FAA field, as far as we know. We emphasize the research proposed after 2005, and focus on evaluating the state-of-the-art work. The goal is to present a novel perspective on FAA and its latest trend.

This paper is organized as follows: Section 2 intro-

duces a generic pipeline of FAA and briefly discusses facial preprocessing methods. Section 3 presents a taxonomy of mainstream graph-based methods for facial representation. Section 4 reviews traditional and advanced approaches of graph relational reasoning and discusses their pros and cons in FAA tasks. The comments of commonly used public FAA databases are given in Section 5. Section 6 summarizes main FAA applications and current challenges based on a detailed comparison of related literature. Finally, Section 7 concludes with a general discussion and identifies potential directions.

2 FACIAL AFFECT ANALYSIS

2.1 General Pipeline

A standard FAA method can be broken down into its fundamental components: facial preprocessing, affective representation and task analysis. As a new branch of FAA, the graph-based method also follows this generic pipeline (see Fig. 2). Regarding the first two steps, many of their approaches can be used and shared when implementing various FAA tasks, while others are coupled with a certain logic according to previous outputs and next goals. Specifically, comparing to other existing FAA methods, the graph-based FAA pays more attention to how to represent facial affects with graph and how to obtain affective features from such representation by graph reasoning. Naturally, depending on different affective graph representation, generic approaches need to be adjusted or new graph-based approaches are proposed to infer the latent relationship and generate the final affective feature. The introducing of graph neural networks (GNNs) is an example. Hence, advantages and limitations of different graph generation methods and their relational reasoning approaches are two main topics of this survey.

2.2 Role of Graph

In mathematical terms, a graph can be denoted as $G = (V, E)$, where the node set V contains all the representation of the entities in the affective graph and the edge set E contains all the relations between two entities. For the sake of computation, the two sets commonly exist in the form of matrices. The edge set E is often represented as an adjacency

matrix A where each element A_{ij} attribute for a degree of relation between the node N_i and N_j . The node set V is represented as the feature matrix H where each vector H_i in H is the feature representation of a node N_i .

Apparently, all the structure information of a graph is contained in E . Thus, when E is empty, G becomes an unstructured collection of entities. Given this unstructured collection, performing relational reasoning requires the model to infer the structure of the entities at a higher order before predicting the property or category of an object. Meanwhile, we could also define some initial graph structure ahead of the relational model, which is a general practice in many affective graph representations. With richer information being manually or automatically provided through prior knowledge, the graph-based FAA methods are expected to exhibit better performance and generalization capability.

2.3 Preprocessing

Face detection is a necessary pre-step before conducting all kinds of FAA. It aims to first locate faces presented in raw images, and then obtain their bounding boxes. Early work usually utilizes Viola and Jones [35], a cascade of weak classifiers, but its performance decreases when facing head-pose variations. Recently, deep learning methods are used for high speed and accuracy. For instance, the Multi-task Cascaded Convolutional Network (MTCNN) exploits a deep cascaded architecture with multi-task strategy that can fast output aligned face and five facial landmarks [36], and is widely used in FAA researches. The *CenterFace* is another the state-of-the-art face preprocessing algorithm, which predicts facial box and landmark location simultaneously [37]. It is more efficient than MTCNN when handling multi-subject face images, and thus suitable for images under complex conditions. The reader is referred to [38] for an extensive review on face detection methods.



Fig. 3. An illustration of face detection and face registration. The *happy* image is from CK+ database [39].

Once the bounding box is located, it is already enough for some FAA method to perform feature learning. However, one additional procedure called face registration is meaningful to improve the FAA performance [40], [41]. With this step, facial landmarks or face geometry are obtained to transform an input face into a prototypical face, which normalizes face variations and corrects the in-plane rotation. Although several methods (e.g., MTCNN & *CenterFace*) deal with face detection and face registration at the same stage, a transformation computed from more landmarks can be more comprehensive and less sensitive to individual landmark errors, which is crucial for graph-based affective representation. The Active Appearance Models (AAM) is one of

the classic methods for both whole face and parts (e.g., eyes, nose, mouth) registration [42]. However, the performance of AAM decreases heavily in real-world scenarios including head-pose variations and partial occlusions. To this end, mixtures of Trees (MoT) [43], a popular part-based face registration method, is employed to cope with in-the-wild conditions [44]. Alternatively, some cascaded deep models with real-time performance are drawing attentions in recent years [45], [46]. Unsupervised approaches such as Supervision by Registration and Triangulation (SRT) [47] are also explored for enhanced landmark detection in multi-view images and videos. Figure 3 presents an illumination of the preprocessing steps. A thorough review on this subject is out of the scope of this paper, the reader is referred to [48], [49] for more details.

3 GRAPH-BASED AFFECTIVE REPRESENTATIONS

Affective representation is a fundamental procedure for most graph-based FAA methods. Depending on the domain that an affective graph models, we categorize the representation strategies as spatial graph, spatio-temporal graph, AU-level graph and others. Figure 4 illustrates a detailed summary of literature using different graph representations. Note that many graph-based representations contains pre-extracted geometric or/and appearance features. These feature descriptors, no matter hand-crafted or learned, are not essentially different from those used in non-graph-based affective representations. Interested readers can also refer to [4], [27], [30] for a systematic understanding of this topic.

3.1 Spatial Graph Representations

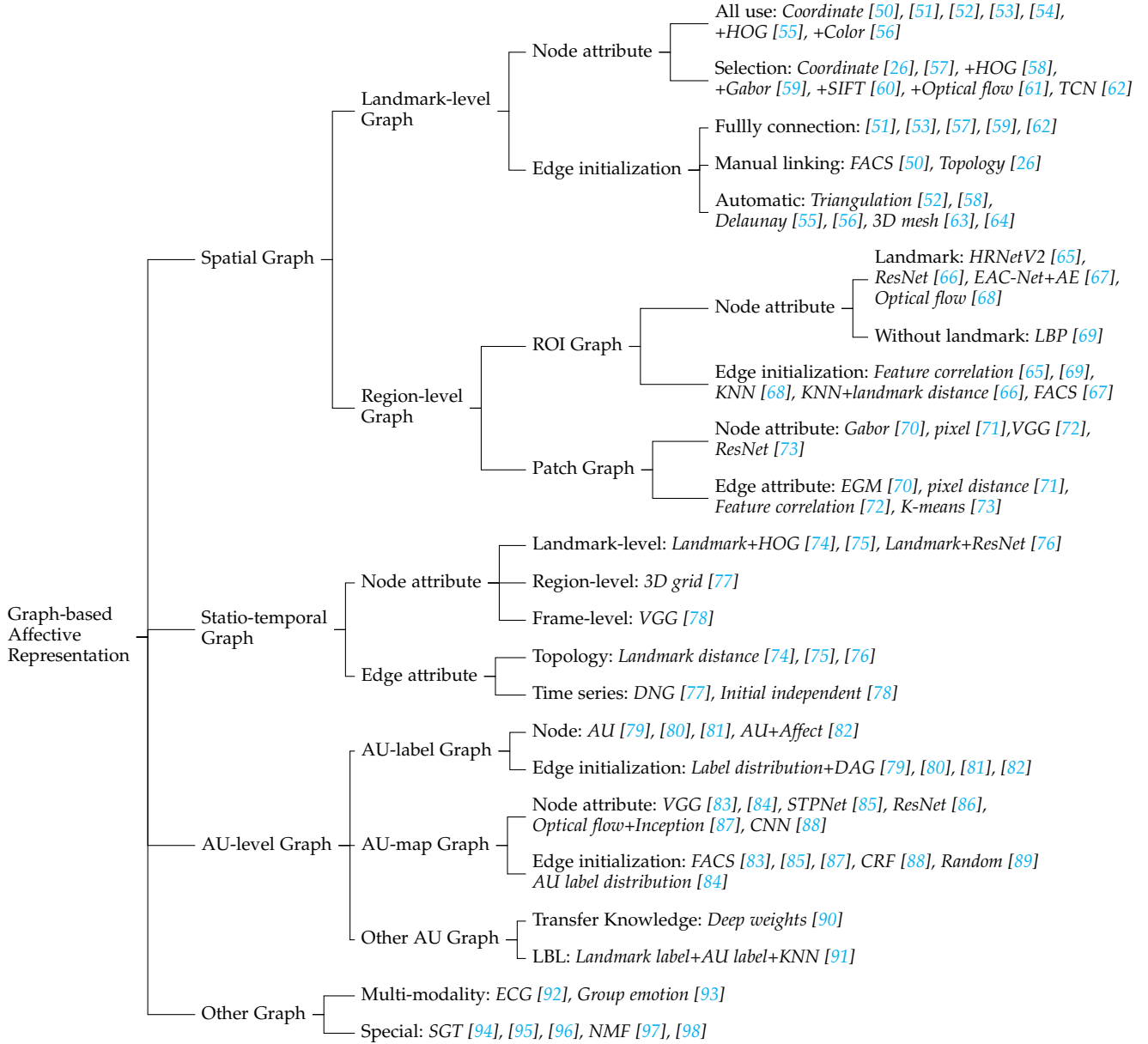
Spatial representations aim to encode facial geometry or appearance from an affective face. Generic spatial methods treat a facial affect as a whole representation or pay attention to variations among main face components or crucial facial parts [99], [100], [101]. For graph-based spatial representations, not only facial changes are considered, but also their co-occurrence relationships and affective semantics are regarded as important cues for FAA [59], [62], [69]. The approaches used to generate spatial affective graphs can be divided into landmark-level graphs and region-level graphs. Figure 6 illustrates frameworks of different spatial graph representations.

3.1.1 Landmark-level graphs

Facial landmarks are one of the most important geometric information that reflects the shape of face components and the structure of facial anatomy. An illustration is shown in Fig. 5. Thus, it is a natural idea to use facial landmarks as base nodes for generating a graph representation. Note that facial shape is not the only information that landmark-level graphs encodes, facial appearances like color [56] and texture [60] are also exploited to enrich landmark-level graphs.

Limited by the performance of landmark detection algorithms, only a few landmarks are applied in early graph representations. Tanchotsrinon *et al.* [50] constructed a facial graph based on 14 landmarks located at regions of (inner/middle/outer) eyebrows, (inner/outer) eyes and

Fig. 4. Taxonomy for Graph-based Facial Representation.



mouth. Similarly, Durmuşoğlu *et al.* [51] utilized 18 landmarks to describe the geometric information related with basic face components. Recently, graph representations using more facial landmarks are proposed to depict fine-grained facial shapes. Sabzevari *et al.* [52] introduced constrained local model to search 60 related facial landmarks and then establish a similarity normalized graph with a raw vector of landmark coordinates. The 68 landmarks detected by *dlib* library [102] or the 66 landmarks provided by *AAM* are also widely used to construct facial graph. For example, in [55] and [53], authors associated the 68 landmarks with the AUs in FACS and made graph-based representations. The difference is that the former additionally employed local appearance features extracted by Histograms of Oriented Gradients (HOG) [103], [104] as attributes of nodes, while the latter proposed two strategies, *full-face graph* and *FACS-based graph*, for enhanced geometric representations.

Specially, Kaltwang *et al.* [54] formulated a Latent Tree (LT) where 66 landmarks were set as part of leaf nodes accompanying by several other leaf nodes of AU targets and hidden variables. This graphical model represented the joint distribution of targets and features that was further revised through conducting graph-edits for final representation.

Furthermore, some current methods exploit landmark selection to avoid the information that is not related to facial affects. Landmarks locating external contour and nose are frequently discarded [26], [58] (see Figs. 6a, 6b). Sechkova *et al.* [60] and Zhong *et al.* [59] chose to remove the landmarks of the facial outline and applied a small window around each remaining landmarks as graph node, while the local features were extracted by Scale Invariant Feature Transform (SIFT) [105] and Gabor filter [106] respectively. As mentioned at the beginning, since these local patches were segmented to introduce facial appearance into the graph

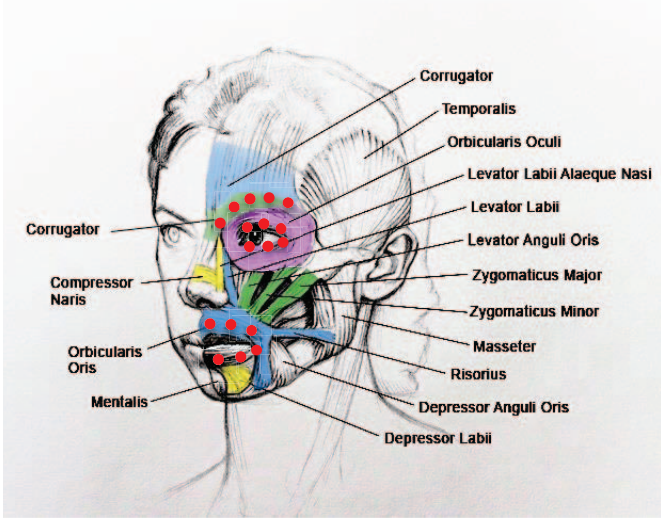


Fig. 5. Facial expression muscle anatomy and related landmarks [26].

representation rather than as independent nodes, similar to [55], we still classify them in landmark-level graphs. For a more extreme instance, authors in [62] only used 28 landmarks of the eyebrows and mouth areas that had significant contributions to micro-expressions. By doing this, it could increase focus on muscle movements that might occur during displaying a facial affect. On the other hand, in order to build more comprehensive graph representations, strategies based on FACS have been designed to select reasonable landmarks. Hassan *et al.* [57] picked out landmarks that indicated both ends of eyebrows, eyes, nose, mouth, upper and lower lips, plus with two points on each side of the face contour (in total 20 landmarks). Then the generated facial graph could keep an appropriate dimension and represent sufficient affective information.

In addition, edges are another key elements that cannot be ignored in graph definition. In the case of landmark-level graphs, a fully connected graph is the most intuitive way to form edges [51], [53], [57], [59], [62]. However, the number of edges is $n(n-1)/2$ for a complete graph with n nodes, which means the complexity of the spatial relationship will increase as the number of nodes increases. This positive correlation is not so correct in analyzing facial affects. For example, assuming the left eyebrow has five landmarks, the edge connecting adjacent landmarks or landmarks at both ends is obviously helpful. By contrast, links between other non-adjacent nodes seem not that necessary. Since the various parts of the eyebrow mostly move in concert when displaying facial affects, the changing trends contained in these edges are redundant. To this end, researches like [50] and [26] manually reduced edges based on knowledge of muscle anatomy and FACS, with results of 21 edges of 14 landmarks and 53 edges of 50 landmarks respectively. Another type of approaches is to exploit triangulation algorithms [52], [58], such as *Delaunay* triangulation [56], to generate edges of a facial graph. The triangular patches formed by landmarks are consistent with true facial muscle distribution and edges are uniform for different subjects [55]. Similarly, the landmark-level graph representation with triangulation is also utilized in generating sparse or dense

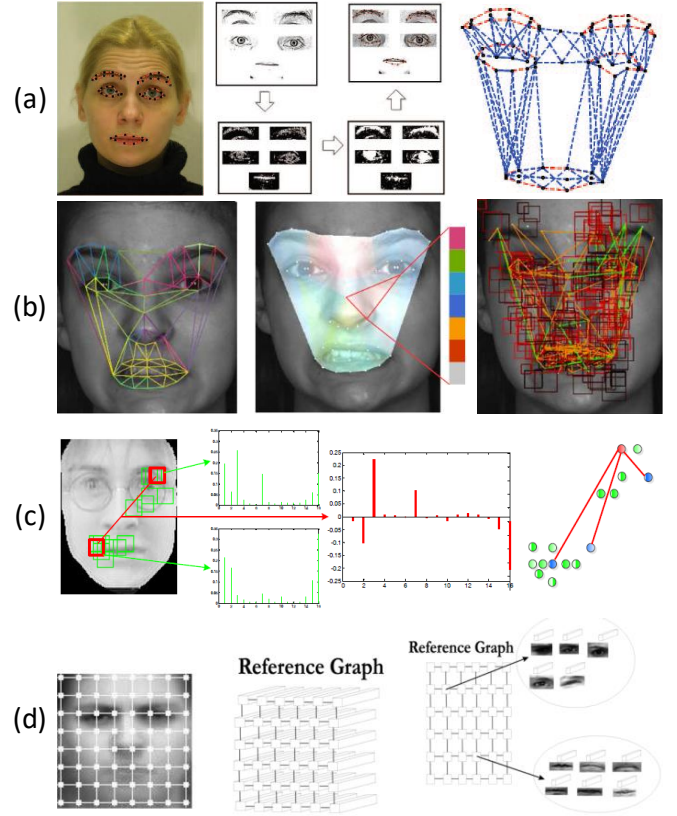


Fig. 6. Spatial graph representations. (a) Landmark-level graph with FACS-based edges [26]; (b) Landmark-level graph with automatic triangle edges [58]; (c) ROI graph with edges computed based on correlation [69]; (d) Patch graph with individual nodes [70].

facial mesh for 3D FAA [63], [64]. For edge attributes of these facial graphs, the *Euclidean* distance is the simplest and most dominant metric, even with multiple normalization methods including diagonal line [50], inner-eyes distance [55] and maximum distance [57]. The gradient computation [53] and hop distance [74] have also been explored as edge attributes to model spatial relationship in different levels. Apart from aforementioned edge connection strategies, several learning-based edge generation methods (e.g., Bayesian method [52], LT [54], Conditional Random Field [88]) have been proposed to automatically extract semantic information from facial graphs. This part is discussed in detail in Sec. 4.1 and 4.4.

3.1.2 Region-level graphs

Region-level representations usually describe faces in terms of individually local areas and thereby ignore the spatial relationships among facial components. To solve this shortcoming, using graph structure to encode the spatial relations into the region-level representation is intuitive. Although many graph-based representations can be constructed in a region-level manner, there are two main categories of affective graphs: region of interest (ROI) graphs and patch graphs.

ROI graphs partition a set of specific facial areas as graph nodes which are highly related to affective display. Coordinates of facial landmarks are commonly applied to locate and segment ROIs. Unlike some landmark-level graph

representations that only use texture near all landmarks as supplementary information, ROI graphs explicitly select meaningful areas as graph nodes, and edges do not entirely depend on established landmark relationships. Zhang *et al.* [65] built mappings between 24 ROIs and 12 AUs, and then selected representative landmarks that spotted ROI centers according to descriptions in FACS. Next, the authors introduced the idea of heatmap and employed the *HRNetV2* [107] as the backbone network to regress the ROI maps. Each spatial location in the extracted feature map were considered as one node of the facial graph, while edges were induced among node pairs. Similarly, Fan *et al.* [66] pre-defined the central ROI locations based on facial landmarks and utilized feature maps of ROIs outputted by the *ResNet-50* [108] as nodes to construct a K-Nearest-Neighbor (KNN) graph. For each node, its pair-wise semantic similarities were calculated, and the nodes with the closest *Euclidean* distance were connected as initial edges. Another example is in [68], Liu *et al.* employed the Main Directional Mean Optical-flow (*MDMO*) [61] as node attributes of 36 ROIs segmented based on 66 landmarks. And a KNN graph was generated in *MDMO* space to encode the local manifold structure for a sparse representation. Due to that different AUs might occur at the same location, Liu *et al.* [67] firstly defined 12 shared local ROIs and one global ROI by taking FACS and landmarks as reference. Subsequently, the *EAC-Net* [109] was exploited to refine the location of ROIs, and each ROI was then fed into an Auto-Encoder (AE) to obtain its latent vector, which was regarded as the node attribute. In addition, the method of obtaining ROIs without relying on facial landmarks has also been studied. Yao *et al.* [69] proposed a pair-wise learning strategy to automatically discover regions that were in part consistent with the locations of AUs (see Fig. 6c). The Local Binary Pattern (*LBP*) histograms [110] of the learned facial regions and their feature correlations were taken as node and edge attributes of an undirected graph (either fully connected or highly sparse) respectively to construct two discriminative representations.

Different from ROI graph representations, the graph nodes in patch graphs are local areas evenly distributed or partitioned in a fully automatic manner from raw face images without manual prior guidance. Zafeiriou *et al.* [70] created a reference bunch graph by evenly overlaying a rectangular graph on object images (see Fig. 6d). For each node of the graph, Normalized Morphological Multi-scale Analysis (*NMMA*) based on *Gabor* filters [111] was designed to compute a set of feature vectors for different facial instances. The structure of the graph representation was optimized by solving an Elastic Graph Matching (*EGM*) problem which is discussed in Sec. 4.4. Such grid derived graph representation was also applied in [71]. Each pixel of the image was set as one node of an undirected graph, while every node was connected to pixels at a *Euclidean* distance below a certain threshold. Recently, several graph representations try to introduce regions beyond facial parts or single face image as context nodes. Zhang *et al.* [72] exploited the *RPN* [112] with a backbone of *VGG16* [113] to extract feature vectors from 10 regions including both the target face and its contexts. The affective relationship between every two nodes were calculated based on the

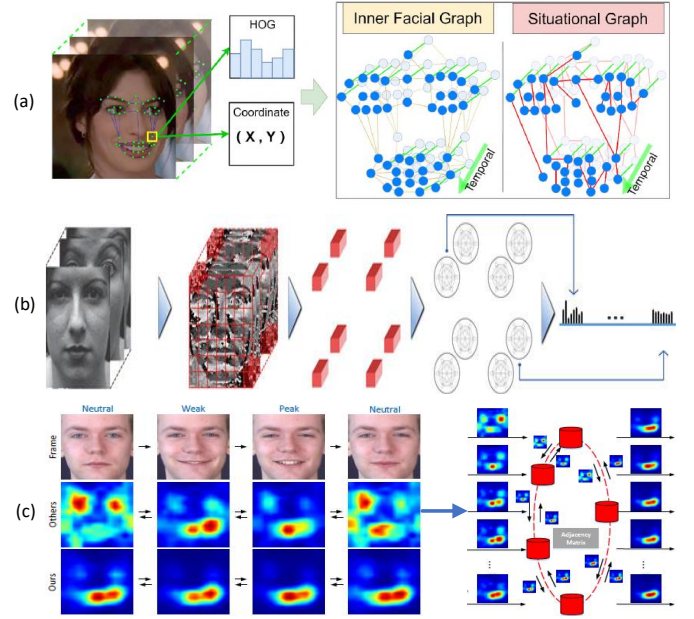


Fig. 7. Spatio-temporal graph representations. (a) Landmark-level graph with adaptive edges [75]; (b) Region-level graph with edges computed based on transitional masks [77]; (c) Frame-level graph with learned edges [78].

feature vectors to generate graph edges. Xie *et al.* [73] built two graph representations for cross-domain FAA. Holistic and local feature maps (eyes, nose, mouth corners) were firstly extracted from corresponding regions by *MTCNN* [36] and *ResNet-50* [86] for both the source domain and the target domain. Then, three type of connections, global-to-global connection, global-to-local connection and local-to-local connection were computed according to statistical feature distribution acquired by *K-means* algorithm and fine-grained iterative update. They were further used to initialize the corresponding graph nodes and establish intra graph and inter graph respectively.

3.2 Spatio-Temporal Graph Representations

Literally, spatio-temporal representations deal with a sequence of frames within a temporal window, and can describe the dynamic evolution of facial affects, especially those subtle affective variations (e.g., eye blinking). In particular, introducing temporal information allows nodes in different static graphs to interact with each other, and generates a more complex graph representation of affective face. Figure 7 presents frameworks of different spatio-temporal graph representations.

Most existing approaches choose to extend the spatial graphs to the spatio-temporal domain. Rivera *et al.* [77] first chose a *Kirsch* compass mask [114] to obtain the directional number response of each facial grid in eight different directions, while a 3D *Gaussian-like* weighted compass mask gave nine space-time directional edge responses corresponding to each of the symmetry planes of a cube. The 2D and 3D masks provided facial information for a given local neighborhood, and were then used as nodes to define a spatio-temporal Directional Number Transitional Graph (*DNG*). Such weighted and directed graph could represent salient

changes and statistic frequency of affective behaviors over time (see Fig. 7b). Several representations defining temporal connections between landmarks in adjacent frames have been proposed, which can be regraded as landmark-level spatio-temporal graphs. Zhou *et al.* [74] developed a spatial temporal facial graph with selected facial landmarks attributed by HOG and XY coordinates as nodes. The intra-face edges were initialized based on semantic facial structure, while the inter-frame edges were created by linking the same node between consecutive frames. Similar landmark-based edge initialization in temporal domain was also utilized in [76]. In the extended work [75] of [74], the authors introduced a connectivity inference block, called Situational Link Generation Module (SLGM), that could automatically generate dynamic edges to construct a spatio-temporal situational graph for a representation of part-occluded affective face (see Fig. 7a). Not like aforementioned landmark-level graphs, Liu *et al.* [78] first extracted a holistic feature of each frame by VGG16 [113] and set them as individual nodes to establish a fully connected graph (see Fig. 7c). And the edge connections would be updated during learning long-term dependency of nodes in time series, which could be seen as a frame-level graph representation.

3.3 AU-level Graph Representations

Although the knowledge of AUs and FACS are used in the above two types of affective graphs, many graph representations have been proposed to model affective information from the perspective of AUs themselves. We divide these approaches into two categories: AU-label graph and AU-map graph. Figure 8 shows frameworks of different AU-level graph representations.

3.3.1 AU-label graphs

Different from spatial or spatio-temporal representations, AU-label graphs concentrate on building an affective graph from the label distribution of training data. Tong *et al.* [79] computed the pair-wise co-occurrence and co-absence dependency between two AUs from existing facial affect database (see Fig. 8a). Since the dependency of any two AUs is not always symmetric, these relationships of AU labels were used as edges to construct an initial Directed Acyclic Graph (DAG). Similarly, Zhu *et al.* [80] followed the definition of DAG and maximized the Bayesian Information Criterion (BIC) score function to learn the graph structure. In [81], an AU-label graph was built with a data-driven asymmetrical adjacency matrix that denoted the conditional probability of co-occurrence AU pairs. The initial dependent representation of each AU would be set as learnable weights of the spatio-temporal features outputted by a 3D-ResNet-18 [115] to generate ultimate predictions. On the other hand, Cui *et al.* [82] established a DAG where object-level labels (facial affect category) and property-level labels (AU) were regarded as parent nodes and child nodes respectively. The conditional probability distribution of each node to its parents was measured to obtain graph edges for correcting existing labels and generating unknown labels in large-scale FAA databases.

3.3.2 AU-map graphs

Judging from the elements used in a graph construction, the AU-map graph is very close to some region-level spatial representations. Because they all employ regional features as the attribute of graph nodes, but AU-map graphs further extract the feature maps that represents corresponding AUs. Similar to ROI graphs, Li *et al.* [83] first extracted a multi-scale global appearance feature with VGG19 [113] and cropped it into several ROI regions based on landmark locations to learn 12 AU features. These learned AU features and the AU relationships gathered from both training data and manually pre-defined edge connections [116] were combined to construct a knowledge graph (see Fig. 8b). The homologous protocol was also conducted in [85] and [87], the former utilized STPNet [117] followed by global average pooling to obtain corresponding AU features of graph nodes, while a Dual-Inception [118] network with optical flow images as input was exploited in the latter. Some special AU-map graphs have been proposed to introduce structure learning for more complex FAA tasks. Walecki *et al.* [88] trained a Convolutional Neural Network (CNN) to jointly learn deep facial features from multiple databases. And these corresponding individual AU features were then used to represent graph nodes. The *copula functions* [119] was applied to model pair-wise AU dependencies in a Conditional Random Field (CRF) graph. To account for indistinguishable affective faces, Corneanu *et al.* [84] designed a VGG-like patch prediction module plus with a fusion module to predict the probability of each AU. A prior knowledge taken from the given databases and a mutual gating strategy were used simultaneously to generate initial edge connections. In order to model uncertainty of AUs in real world, Song *et al.* [89] established an uncertain graph, in which a weighted probabilistic mask that followed Gaussian distribution was imposed on each AU feature map extracted by ResNet18 [86]. By doing this, both the importance of edges and the underlying uncertain information could be encoded in the graph representation.

3.3.3 Other AU graphs

A few approaches of building AU-level graph representations from other aspects have been studied. Niu *et al.* [90] proposed two Deep Neural Networks (DNNs) to extract multi-view AU features for both labeled and unlabeled face images. The parameters of these two DNNs were used as graph nodes to share the latent relationships among individual AUs which were embedded in the AU classifier to assist the semi-supervised AU recognition. Chen *et al.* [91] established two KNN graphs of facial landmarks and AUs separately by using their deep features extracted from the training data. The indexes of both central image and its neighbors were stored in an index-similarity list to boost the Label Distribution Learning (LBL). The generated auxiliary label space graphs followed an assumption that facial images should have nearby distributions to their neighbors in the label space of auxiliary tasks (see Fig. 8c). It was similar to the idea of [82].

3.4 Other Representations

Recently, several graph representations that do not fall into the above categories have been proposed, which indicates

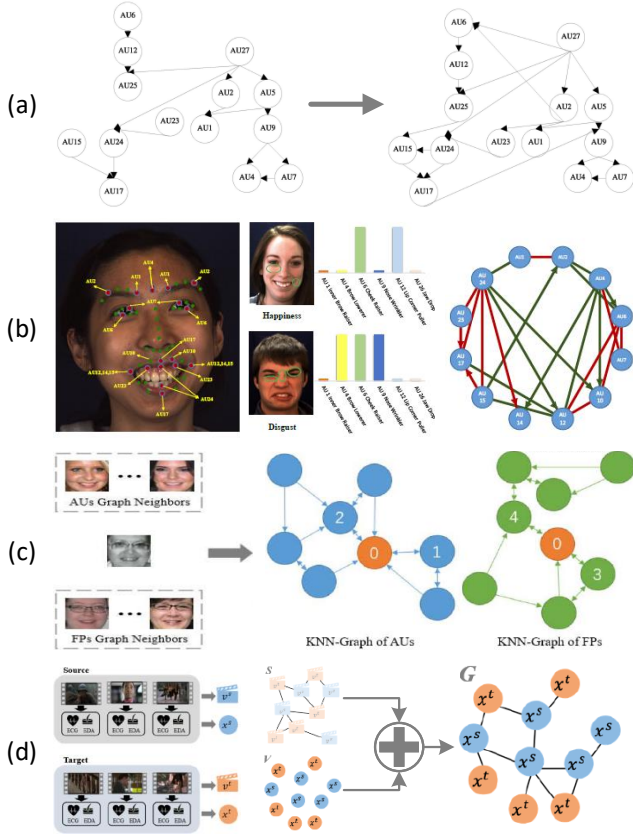


Fig. 8. AU-level and Multi-modal graph representations. (a) AU-label graph with edges generated from training data [79]; (b) AU-map graph with FACS based edges [83]; (c) Auxiliary graphs of both AUs and landmarks [91]; (d) Multi-modal graph of both visual and physiological signals [92].

that this is still an open research field. In order to combine signals from multiple corpus, Chien *et al.* [92] proposed a dual-branch framework, in which the visual semantic features were extracted by a 3D-CNN [120] in both source and target sets. These features were then retrieved with *Spearman* correlation coefficient to generate positive edge connections in the manner of cross corpus (see Fig. 8d). Such learnable visual semantic graph could be used to perform training and prediction by masking nodes of induced Low-level Physiological Descriptors (LLDs) of different sets respectively. Xu *et al.* [93] built an emotion-based directed graph according to label distributions of facial affects in existing training data. Specifically, its nodes were initialized word vectors of the corresponding emotions, while the edges represented conditional probabilities of pair-wise emotions. The learned local relationship patterns could be injected into a network at the feature level to enhance the performance of final multimedia affect tagging.

Besides, some special graph representations of FAA such as Spectral Graph Transform (SGT) [94], [95], [96] and Non-negative Matrix Factorization (NMF) [97], [98] have also been explored.

3.5 Discussion

As an important part of graph-based FAA, there is a certain causal relationship between the choice of graph representa-

tion methods and the selection of relational reasoning methods. The spatio-temporal graph and the AU-level graph are most notable recent trend of graph-based facial representations. And the limitations of these three types are discussed as follows.

Spatial graph representations: Conceptually, landmark-level graphs have certain limitations from both externally and internally. On one hand, most of the generated graphs are sensitive to detection accuracy of facial landmarks, thereby may fail in uncontrolled conditions. On the other hand, the selection of landmarks and the connection of edges have not yet formed a standard rule. Although some FACS-based strategies have been designed, the effects of different landmark sets and different edge connections on the graph representation are rarely reported. Finally, recent trend of developing FAA methods is to combine every procedure as an end-to-end learning pipeline. Thus, how to integrate the process of establishing landmark-level graphs into existing frameworks still needs to be studied.

Comparing with landmark-level graphs by modeling the facial shape variations of fiducial points, region-level graph representations explicitly encode the appearance information in local areas. And the spatial relationships among selected regions are measured through feature similarity instead of manual initialization based on facial geometry. The graph reasoning will be the next step to learn task-specific edge connections and discriminative affective features using techniques such as CNNs [121] or Graph Neural Networks (GNNs) [122], which are discussed in Sec. 4. The two types of region-level graph representations have their own characteristics, but have some flaws as well. For the ROI graphs, the circumstance resulting from inaccurate or unreasonable landmarks will also have an impact on some related representations. In addition, the contribution of geometric information for FAA has proven in [99], thereby should be more effectively integrated into ROI graph representations. For patch graphs, incorporating context regions or multiple face regions into graph nodes is an emerging topic. Due to that most existing approaches utilize a region searching strategy, the problem is how to avoid the loss of target face and how to exclude invalid regions. Besides, as far as the literature we have collected, there is no work on combining the ROI graph and patch graph to construct a joint graph representation, which we think is a promising direction.

Spatio-temporal graph representations: In spite of the advantage of extra dynamic affective information in spatio-temporal graph representations, there are several drawbacks in existing approaches. For landmark-level graphs, the current initialization strategy of edge connections is simply to link the facial landmark of the same index frame by frame. No research has been reported to learn the interaction of landmarks with different indexes in the temporal dimension. Besides, in addition to *Euclidean* distance and *Hop* distance, other edge attributes measurement methods should also be explored to model the semantic context both spatially and temporally. For the frame-level graph, the domain knowledge related to affective behaviors like muscular activity that can be embedded with graph structure is not explicitly considered in recent work. Therefore, building a hybrid spatio-temporal graph is a practical way to encode

the two levels of affective information at the same time.

AU-level graph representations: Most AU-label graphs rely on the label distributions of one or multiple given databases. One problem is the available AU labels because not every public databases provides the annotated AU label. In addition, since AU labeling requires annotators with professional certificates and is a time-consuming task, existing databases with AU annotations are usually small-scale. Therefore, the distribution from limited samples may not reflect the true dependencies of individual AUs. To address this demand, some semi-supervised methods are introduced based on underlying assumptions like the potential mapping between facial affect categories and AUs. However, the reliability of this hypothesis is questionable when faced with complex FAA tasks including micro-expression recognition and continuous affect prediction. Another problem is that the measurement criteria of AU correlations are versatile but not general for both AU-label graphs and AU-map graphs, and can result in different initialized AU dependencies. The impact of these measurements on FAA still needs to be evaluated.

4 AFFECTIVE GRAPH RELATIONAL REASONING

The relational reasoning is the other significant procedure for graph-based FAA methods. The ability to reason about the relations between entities and their properties is believed to be the crucial step towards actual intelligence for machine learning systems [123]. Such a mechanism can be considered as a two-step process, i.e., understanding the structure from a certain group of entities and making inference of the system as a whole or the property within. Consequently, a model that is able to perform relational reasoning has to output the structure as well as the property of the unstructured entity set. However, things are slightly different in the case of graph-based FAA. Depending on what kind of affective graph representation is exploited, the contribution of graph relational reasoning can be either merged at the decision level with other affective features, or reflected as a collaborative way in the level of feature learning. In this Section, we review relational reasoning methods designed for affective graph representations in four categories: dynamic Bayesian networks, classical deep models, graph neural networks and other machine learning techniques.

4.1 Dynamic Bayesian Network

Dynamic Bayesian Networks (DBNs) are models mostly used to capture the relationships in AU-label graph representations. The Bayesian Network is a Directed Acyclic Graph (DAG) that reflects a joint probability distribution among a set of variables. In the DAG, nodes indicate variables and the connections among the nodes represent the conditional dependency among variables. In the work of [79], a DAG was manually initialized according to prior knowledge, then larger databases were used to perform structure learning to find the optimal probability graph structure. After the optimal graph structure was obtained, the probabilities of different AUs were inferred by learning the DBN. Following this idea, Zhu *et al.* additionally integrated DBN to a multi-task feature learning framework and

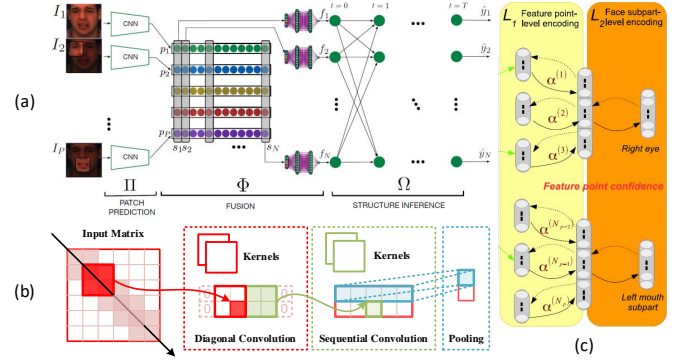


Fig. 9. Classical deep models for graph learning. (a) RNN [84]; (b) CNN [55]; (c) AE [58].

made the AU inference by calculating the joint probability of each category node. Another advanced research of DBN is [82]. The inherent relationships between category labels and property labels were modelled by a DBN. And the DBN parameters were utilized to denote the conditional probability distribution of each AU given the facial affect. The wrong labels could be corrected by leveraging the dependencies after the structure optimization.

4.2 Adjustments of Classical Deep Model

Before the graph neural network is widely employed, many studies have adopted conventional deep models to process affective representations with the graph structure. These deep models are not specifically designed but is able to conduct standard operations on graph structural data by adjusting the internal architecture or applying additional transformation to the input graph representation. Figure 9 shows examples of classical deep models for graph learning.

4.2.1 Recurrent neural network

The variant of Recurrent Neural Networks (RNNs) is one of the successful extension model types for handling graph structural inputs. Similar to random walk, Zhong *et al.* [59] applied a Bidirectional Recurrent Neural Network (BRNN) to deal with its landmark-level spatial graph representation in a rigid order. To incorporate the structural information represented by Euclidean distance, the extracted Gabor feature of each node in the graph was updated by multiplying with the average of the connected edges. Subsequently, the nodes were iterated by a BRNN with learnable parameters in both the forward and the backward direction. And the outputs were further fed to a fully-connected (FC) layer and a softmax layer for facial affect classification. In the work of [84], the authors built a structure inference module to capture AU relationships from an AU-map graph representation. Based on a collection of interconnected recurrent structure inference units and a parameter sharing RNN, the mutual relationship between two nodes could be updated by replicating an iterative message passing mechanism with the control of a gating strategy (see Fig. 9a). And the final messages and previous individual AU estimations were combined to produce advanced AU predictions.

4.2.2 Convolutional neural network

Different from the sequential networks, Liu *et al.* [55] utilized a variant CNN to process the landmark-level spatial affective graph. Compared to standard convolution architectures, the convolution layer in this study convolved over the diagonal of a special adjacency matrix so that the information can be aggregated from multiple nodes. Then a list of the diagonal convolution outputs was further processed by three sequential convolution layers which are 1-D convolution. The corresponding pooling processes were performed behind convolution operations to integrate feature sets (see Fig. 9b). Predictions of facial affects were outputted by FC and *softmax* layers. Another attempt for landmark-level spatial graph representations is the *Graph-TCN* [62]. It followed the idea of *TCN* residual blocks that consisted of standard convolution, dilated casual convolution and weight normalization [124]. By using different dilation factors, *TCNs* were applied to convolve the elements that are both inside one node sequence and from multiple node sequences. Thus, the *TCN* of a node and *TCN* of an edge could be trained respectively to extract node feature and edge feature at the same time. Besides, Fan *et al.* exploited a Semantic Correspondence Convolution (SCC) module to model the correlation among its region-level spatial graph. Based on an assumption that the channels of co-occurrence AUs might be activated simultaneously, the Dynamic Graph Convolutional Neural Network (DG-CNN) [125] was applied on the edges of the constructed KNN graph to connect feature maps sharing similar visual patterns. After the aggregation function, affective features were obtained to estimation AU intensities.

4.2.3 Auto-Encoder network

The approach of AEs has also been explored. Dapogny *et al.* [58] employed a hierarchical auto-encoder network to capture the relationship from the constructed landmark-level spatial graph. Specifically, the first stage learned the texture variations based on the extracted HOG features for each node. While the second stage accumulated features of multiple nodes whose appearance changes were closely related and computed the confidence scores as the triangle-wise weights over edges (see Fig. 9c). Finally, a Random Forest (RF) was used for facial affect classification and AU detection simultaneously.

4.3 Graph Neural Network

Not like conventional deep learning frameworks mentioned in Sec. 4.2, GNNs are proposed to extend the 'depth' from 2D image to graph structure and established an end-to-end learning framework instead of additional architecture adjustment or data transformation. Several types of GNNs have been successfully used to address the relational reasoning of affective graph representations in FAA methods.

4.3.1 Graph convolutional network

Graph Convolutional Networks (GCNs) [126] are the most popular GNN in graph-based FAA researches. In general, there are two ways to perform graph convolution, i.e., the spatial GCN or the spectral GCN. Due to the flexibility of extending graph-scale and the potential for parallel

computation, the spatial approach is more frequently used. Figure 10 illustrates several GNN architectures for relational reasoning.

Practically, GCN can be set as an auxiliary module or part of the collaborative feature learning framework. For the former, GCNs are applied immediately after the graph representation. However, the outputs of relational reasoning are not directly used for facial affect classification or AU detection, but are later combined with other deep features as a weighting factor. In *MER-GCN* [81], the AU relationships were modelled by the conditional probability in an AU-label graph representation. Each node was represented as a one-hot vector and fed into a GCN to perform node dependency learning. The generated graph features were embedded to the sequence level deep feature together for final classification. Similarly, Niu *et al.* [90] employed a two-layer GCN for message passing among different nodes in its AU-level graph. Both the dependency of positive and negative samples were considered and used to infer a link condition between any two nodes. And the output of GCN was formulated as weight matrix of the pre-trained AU classifiers. Zhou *et al.* [87] performed relational reasoning with GCN that provided an updated relational graph feature for each graph node by aggregating features from all neighbors based on edge weights (see Fig. 10a). Besides, GCNs can also be utilized following the above manner to execute relational reasoning on atypical graph representations, such as multi-target graph [72], cross-domain graph [73] (see Fig. 10b) and distribution graph [127].

For the collaborative framework, GCNs usually inherit the previous node feature learning model in a progressive manner. Like in [67], a GCN-based multi-label encoder was proposed to update features of each node over a region-level spatial graph representation. And the reasoning process was the same as that in the auxiliary framework. Similar studies also include [65] and [92] (see Fig. 10c). In addition, to incorporating the dynamic evolution in spatio-temporal graph representations, Liu *et al.* [78] set GCNs as an imitation of attention mechanism or weighting mechanism to share the most contributing features explore the dependencies among frames. After training, the structure helped nodes update features based on messages from the peak frame and emphasize the concerned facial region. A more feasible way is to apply *STGCN* [128] on spatial-temporal graph representations [74], [76]. In their relational reasoning, features of each node were generated with its neighbor nodes in current frame and consecutive frames by using spatial graph convolution and temporal convolution respectively. To make inference of the node relation in a more dynamic manner instead of using a constant graph structure, Zhou *et al.* [75] proposed an additional network module to adaptively generate conditional edges. Based on the spatio-temporal graph representation, the authors introduced a situational graph generation block that predicted the probability of a link between any two nodes (see Fig. 10d). This block was trained by the mean-square loss over the actual change degree of each link, so that the additional connections reflect the categorical information and are closed to the actual facial variations.

Alternatively, the approach of spectral GCN [129] has also been studied. Wu *et al.* [71] perform the relational

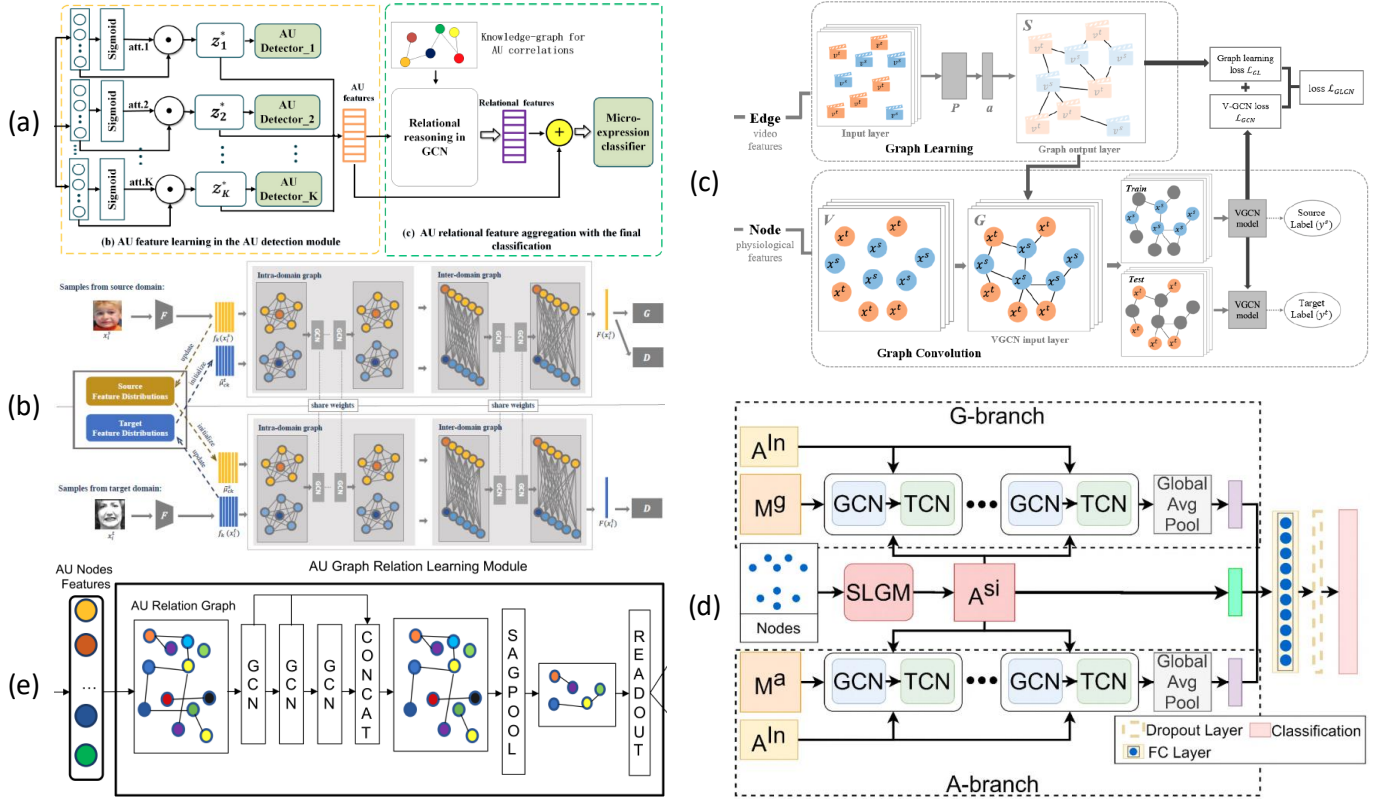


Fig. 10. Graph neural networks for relational reasoning. (a) GCN as auxiliary module [87]; (b) GCN for atypical graph representation [73]; (c) GCN as collaborative framework [92]; (d) STGCN for spatio-temporal graph representation [75]; (e) GAT [85].

reasoning on a patch-level spatial graph representation by using graph convolutions in frequency domain. Each GCN block contained a graph signal filtering layer and a graph coarsening layer. Every two matched nodes were merged into a new node, and the weights of new node was the sum of the weights of two matched nodes. By repeating this operation several times, one FC layer and one *softmax* layer were added for facial affect classification.

4.3.2 Graph attention network

Comparing with GCNs, Graph Attention Networks (GATs) aims to strength the node connections with high contribution and offer a more flexible way to establish the graph structure [130]. Song *et al.* [89] introduced an uncertain graph neural network with GAT as backbone. For its AU-map graph representation, a symmetric weighted mask was employed to characterize the strength of links through parameter update during network training, with an aim to select the useful edges and depress the noisy edges and learn the AU dependencies in the graph for each node. In addition, the underlying uncertainties were considered in a probabilistic way, close to the idea of Bayesian methods in GNN [131], to alleviate the data imbalance by weighting the loss function. Different from directly applying GAT to achieve the attention, Xie *et al.* [85] proposed a graph attention convolutional network that added a self-attention graph pooling layer after concatenating three sequential GCN layers (see Fig. 10e). This improved the reasoning process on an AU-map graph representation, because only important nodes would be left and the aggregated node

features contained contributions of both AU information and facial topology.

4.3.3 Other graph network

According to the structured knowledge graph organized from the AU-map representation, Li *et al.* [83] exploited a Gated Graph Neural Network (GGNN) [132] to propagate node information. Similar to RNNs, it calculated the hidden state of next time-step by jointly considering the current hidden state of each node and its adjacent node. The relational reasoning could be conducted through the iterative update of GGNN over the graph representation. And the GGNN module was further integrated into a multi-scale CNN to embed the globally structured relationships between AUs in an end-to-end framework.

4.4 Basic Machine Learning Model

Although refined deep features extracted by parameterized neural networks and gradient-based methods is the current mainstream, they require a large amount of training samples for effective learning. Due to the insufficient data in early years or the purpose of efficient computation, many non-deep machine learning techniques have been applied for affective graph relational reasoning. Graph structure learning is one of widely used approaches. In [54], the reasoning of its spatial graph representation was conducted by LT learning. Parameters update and graph-edit of LT structure were performed iteratively to maximize the marginal log-likelihood of a set of training data. Walecki *et al.* [88]

employed *CRF* to infer AU dependencies in an AU-map graph. The use of copula functions allowed it easy to model non-linear dependencies among nodes, while an iterative balanced batch learning strategy was introduced to optimize the most representative graph structure by updating each set of parameters with batches. Approaches of graph feature selection are also exploited in this part, including Correlation-based Feature Selection (*CFS*) [51], graph embedding [60], graph sparse coding [68] and frequent subgraphs mining [57]. These above approaches provide a more diverse concept for graph relational reasoning.

4.5 Discussion

The relational reasoning is a significant characteristic of graph-based methods compared to other FAA system. Although different approaches can be exploited to achieve this purpose, drawbacks of the aforementioned four types are discussed as follows.

Dynamic Bayesian network: The vast majority of AU-label graph representations employ *DBNs* as their relational reasoning model. However, the representation quality highly relies on the available training data that need balanced label distribution in both positive-negative samples and categories. This strong demand will limit the effectiveness of node dependencies learned by *DBNs*. While the work about correcting and generating labels based on *DBN* [82] has been proposed, current study has revealed the potential of *GCNs* in processing AU-label graphs. Another problem is that *DBNs* can only be combined with facial features as a relative independent module, and are hard to integrate into an end-to-end learning framework.

Classical deep Model: Standard deep models, including *CNNs*, *RNNs* and *AEs*, have been explored to conduct graph relational reasoning before the emergence of *GNNs*. Even if they are suitable for more graph representations than *DBNs*, the required additional adjustments in input format or/and network architecture make the implementation inelegant. For example, the modification of convolution operations in [55] resulted in losses of node information, while the *RNNs* let node messages only be passed and updated in a specific sequence that suppressed the graph structure [78]. Besides, applying grid models cannot make full use of the advantage of graph. They focus more on local features of the input, but the global property represented by the graph is also very important for the analysis of facial affects. Thus, we think the specific designed networks like *GNNs* will become dominant in this part.

Graph neural network: *GNNs* are developing techniques in relational reasoning. Architectures with different focuses have been proposed, but have their shortcomings as well. For instance, *GCNs* cannot well handle directed edges (e.g., AU-level graphs), while *GATs* only use the node links without the consideration of edge attributes (e.g., spatial graphs). Besides, due to the low dimension of the nodes in affective graphs, too deep *GNNs* may be counterproductive. In addition, being an auxiliary block or part of the whole framework will influence the construction of *GNNs*. Therefore, how to create complementary graph representation and relational reasoning using *GNNs* still needs to be explored.

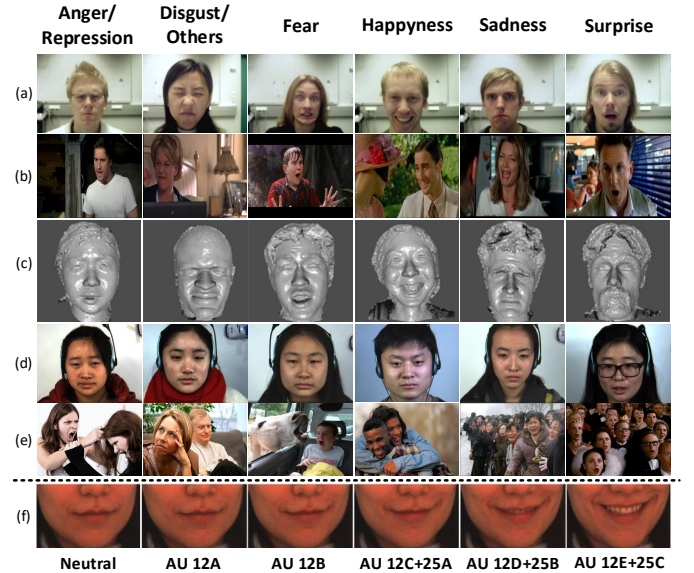


Fig. 11. Facial affect databases. (a) The Oulu-CASIA [133] contains posed facial affects; (b) The SFEW 2.0 [134] has facial affects under in-the-wild scenarios; (c) The BP4D [135] provides 3D affective face images; (d) The CASME II [136] collects images of spontaneous micro facial affects; (e) EMOTIC [137], multiple faces appear in one image with V-A annotations; (f) DISFA [138] offers frame-level AU intensity labels.

Basic machine learning model: Traditional machine learning methods have taken a place in early research. In fact, more advanced techniques like *DBNs* and *GNNs* are partly inspired by them. Nevertheless, one of the reasons they have been replaced is that these approaches need to be designed separately to cope with different graph representations, similar to hand-crafted feature extraction. Hence, it is difficult to form a general framework. On the other hand, larger amounts of training data and richer computing resources allow deep models to perform more effective and higher-order relational reasoning on affective graphs.

5 DATABASES AND VALIDATION

5.1 Databases

Public databases of facial affect are applied as validation material in most FAA studies. Since details of existing databases are different in terms of scales, annotations, sample properties and so on, it provides another perspective to understand current trends of FAA. In this section, we present a comprehensive overview of commonly used databases including latest released ones that have larger data scale and more challenging factors. In addition, with an aim to emphasize on graph-based FAA, we summarize corresponding elements (e.g., landmark coordinates, AU labels) self-carried by databases, which are rarely considered in previous related surveys. In Table 1, the characteristics of these databases are listed from four aspects: samples, attributes, graph-related properties and special contents. Figure 11 exhibits several examples of facial affects under different conditions.

Databases containing posed facial affects are chosen by early FAA methods for validation. The Cohn-Kanade Dataset (CK) [139], Extended CK Dataset (CK+) [39], M&M

TABLE 1
An Overview of Facial Affect Databases

Database/year	Samples			Attributes		Graph-based Properties ⁴				Special Contents ⁵
	Data Type	Subjects	Number	Eli. & Sou. ¹	Affects ²	B.B. ³	LM	AU	Dynamic	
CK(+) [139] ([39]) '10	Sequences	97(123)	486(593)	P & Lab	6B+N(+C)	•	•	• + I	•	/
MMI [39] '10	Images/Videos	75	740/2900	P & Lab	6B+N	◦	◦	•	• + V	Head pose
Oulu-CASIA [133] '11	Sequences	80	2880	P & Lab	6B	•	◦	◦	•	NIR
DISFA [138] '13	Sequences	27	130,000	S & Lab	6B+N	•	•	• + I	• + F	/
FER-2013 [140] '13	Sequences	/	35887	S & Web	6B+N	•	◦	◦	◦	Wild
SFEW 2.0 [134] '15	Images	/	1766	S & Movie	6B+N	•	•	◦	◦	Wild
AFEW 7.0 [141] '17	Videos	/	1809	S & Movie	6B+N	•	•	◦	•	Audio, Wild
BU-3DFE [142] '06	Images	100	2500	P & Lab	6B+N	•	•	◦	◦	3D, Multi-view, I
BU-4DFE [17] '08	Videos	101	606	P & Lab	6B+N	•	•	◦	•	3D, Multi-view
BP4D [135] '14	Videos	41	328	S & Lab	6B+E+P	•	•	•	• + F	3D, Head pose
SMIC [143] '13	Sequences	16	164	S & Lab	3B [†] +N	•	◦	◦	•	Micro., NIR
CASME II [136] '14	Sequences	35	247	S & Lab	3B [†] +R+O	•	◦	•	• + V	Micro.
SAMM [144] '18	Sequences	32	159	S & Lab	6B+C	•	◦	•	• + V	Micro.
CAS(ME) ² [145] '18	Sequences	22	300+57	S & Lab	3B [†] +O	•	◦	•	• + V	Macro. & Micro.
EmotiNet [146] '16	Images	/	950,000	S & Web	6B+17Comp.	•	•	• + I	◦	Wild
ExpW [147] '18	Images	/	91,793	S & Web	6B+N	•	◦	◦	◦	Multi-sub., Wild
RAF-DB [148] '19	Images	/	29672	S & Web	6B+N+11Comp.	•	•	◦	◦	Wild
AffectNet [149] '19	Images	/	420,299	S & Web	6B+N+C+O	•	•	◦	◦	V&A, Wild
EMOTIC [137] '19	Images	/	23,571	S & Web	6B+N+19Comp.	•	◦	◦	◦	V&A, Multi-sub., Wild

¹ Eli.: elicitation; Sou.: source; P: posed; S: spontaneous.

² 6B: 6 basic affects (happiness, sadness, fear, anger, disgust, surprise); N: neutral; C: contempt; E: embarrassment; P: pain; O: others; R: repression; 3B[†]: 3 basic affects (positive, negative, surprise); 3B[‡]: 3 basic affects (happiness, disgust, surprise); Comp.: compound affects.

³ B.B.: bounding boxes; LM: landmarks; • = Yes, ◦ = No.

⁴ I: intensity annotation; V: onset-apex-offset annotation; F: frame-level annotation.

⁵ NIR: near-infrared; Multi-sub.: multiple subjects in one image; Micro.: micro-expression; Macro.: macro-expression; Wild: in-the-wild scenario; V&A: valence and arousal.

Initiative Facial Expression Database (MMI) [150] and Oulu-CASIA NIR&VIS Facial Expression Database (Oulu-CASIA) [133] are the mostly used. And they all provide affective sequences with temporal evolution that are possible to meet requirements of different graph-based representation. A limitation of these four databases is the lack of in-the-wild conditions, which is less challenging for the state-of-the-art methods. Hence, more recent databases such as FER-2013 [140] and Static Facial Expression in the Wild (SFEW) 2.0 [134] tend to acquire more complex affective data from internet or existing digital sources like movies and interviews. Different from the above two databases only providing static images, the Acted Facial Expression in the Wild (AFEW) 7.0 [141] is a temporal version of SFEW with spontaneous facial affects in all kinds of conditions. Moreover, AFEW is also a multi-modal database that provides audio affective data. As a standard database of EmotiW competition, the content of AFEW will be updated synchronously.

Some other databases focus more on affective intensity in addition to discrete facial affects. The Denver Intensity of Spontaneous Facial Action Database (DISFA) [138] contains manually frame-level AU annotations and intensity labels from 0 to 5 for each AU. The Binghamton University 3D Facial Expression Database (BU-3DFE) [142] annotates 6 basic affects with four levels of intensity and provides both 3D facial texture images and geometric shape models. The Binghamton University 4D Facial Expression Database (BU-4DFE) is a dynamic extension of BU-3DFE, which contains multi-view 3D faces but no intensity annotations. The focus on spontaneous affects is also presented in this part. The

Binghamton-Pittsburgh 3D Dynamic Spontaneous Facial Expression Database (BP4D) [135] has both 2D and 3D spatio-temporal videos with facial affects containing head poses. The ground-truth of each AU is annotated frame by frame for 6 basic and 2 non-basic facial affects.

Another type of databases is about micro facial affects (micro-expressions). Different from conventional affective databases, 'reaction' is mainly applied for collecting subtle facial changes. For instance, participants are required to keep a neutral face while watching videos associated with induction of specific affects [151]. Based on this setting, the Spontaneous Micro Facial Expression Database (SMIC) [143], the Chinese Academy of Sciences Micro-expression Database (CASME) II [136] and the Spontaneous Micro-Facial Movement Database (SAMM) [144] are released for micro FAA. Besides, Chinese Academy of Sciences Macro-Expressions and Micro-Expressions Database (CAS(ME)²) [145] is developed for both macro-expressions and micro-expressions. However, due to the time-consuming of data collection and annotation, samples in these micro affective databases are insufficient and distribution imbalanced, and only contain lab-controlled condition.

Recently, several large-scale databases are developed to provide sufficient data with spontaneous facial affects and in-the-wild conditions, especially for FAA methods using deep learning. The Real-world Affective Face Database (RAF-DB) [148] provides nearly 30,000 in-the-wild images with both basic affects and compound affects (e.g., happily surprise, sadly angry). The Large-scale Face Expression in-the-Wild dataset (ExpW) [147] contains 91,793 manually annotated original (without size normalization) web im-

ages. It additionally offers a subset that has multi-subject conditions with interpersonal relation labels. Similar challenging factors can be found in the EMOTIC [137] which has 34,320 annotated faces in 23,571 images. Besides, it also has continuous labels (valence, arousal, dominance) and extra compound emotion classes. AffectNet [149] is the largest existing database with over one million images, while 450,000 of them are manually annotated. And this is currently the biggest large-scale database that provides continuous affective labels (valence and arousal). To avoid time-consuming manual annotation, EmotioNet [146] designed a real-time algorithm to achieve automatic annotation of AUs, AU intensities and affective categories for 950,000 Internet images. Although there is still a certain accuracy gap between manual labels and automatic labels, this is a potential way to efficiently acquire massive labelled affective data.

Through observing the development of facial affective databases, we can conclude an evolutionary FAA path from posed, lab-controlled, conventional to spontaneous view, in-the-wild, and non-basic view. With regard to graph-based FAA, it is available to find and select suitable databases with corresponding metadata, such as landmarks, AU labels and dynamics, for different graph representation purposes. However, existing databases also have some shortcomings. On the one hand, no or not accurate enough AU annotations are provided by in-the-wild databases, which limits the role that AUs can play in FAA. On the other hand, there is still a blank in the field of dynamic large-scale affective database, so that it is hard to use temporal information to generate affective graph representation. Finally, instead of discrete categories, databases about natural and spontaneous facial affects in continuous domain need more attention.

5.2 Evaluation Principle

To fairly testify the performance of FAA methods on public databases, a few standard validation protocols should be followed. The k-fold subject independent cross validation is a widely adopted version. The k-fold crossing operation guarantees the balance of the evaluation result on one database, while the subject-independent rule keeps the testing set isolated during training. A more extreme version is the leave-one-subject-out cross validation, which is usually used in small-scale samples such as micro-expression databases. Since many databases, like SFEW 2.0 [140] and EmotioNet [146], provide official groups of training, validation and testing sets, the holdout validation is also exploited especially in some FAA competitions (e.g., EmotiW [20] and AVEC [23]). Another generic protocol is cross database validation that aims to evaluate the FAA generalization when facing training and testing data from different databases respectively.

The unified metric is another important part of the fair evaluation. One simple but effective metric is average accuracy rate. The F1 score and the area under the receiver operating characteristic (ROC) curve (AUC) are also widely adopted. In addition, the Pearson correlation coefficient and the Intra-class correlation (ICC(3,1)) are two common continuous metrics. The former measures relative differences between target and prediction (similar metrics also include mean squared error (MSE) and mean absolute error (MAE)), while the ICC(3,1) is used in behavioral science to measure agreement between annotators (e.g., AU intensity labels).

Although there are standard validation protocols and unified metrics, the results of different FAA methods can be hardly compared against each other directly due to the different experimental configurations in terms of pre-processing approaches or data grouping strategies. Therefore, some benchmarks based on public databases need to be studied in the future.

6 APPLICATIONS AND PERFORMANCE

According to different description models of facial affects, the FAA can be subdivided into multiple applications. Typical output of FAA systems is the label of a basic facial affect or AUs. Recent researches also extend the goal to predict micro-expression or affective intensity labels or continuous affects. In this Section, we compare and discuss the graph-based FAA methods presented in this paper from three main application categories: facial expression recognition, AU detection, and micro-expression recognition. Some special studies outside these three will also be evaluated.

6.1 Facial Expression Recognition

Facial expression recognition (FER), also known as macro-expression recognition, has been working on the topic of basic facial affects classification. A certain trend of FER is that the research focus has shifted from the early posed facial affects in controlled conditions to the recent spontaneous facial affects in real scenarios. In other words, the recognition of the former is considered as a solved problem for FAA methods including graph-based FER, which can be corroborated from the results in Table 2. For example, the performance on CK+ database is very close to 100% [64], [71], [77], [78].

From the view of the representation, spatial graphs and spatio-temporal graphs are dominant in graph-based FER methods. The only exception is [91] where the authors utilized the auxiliary label space graphs of the landmark detection and AU detection to approximately learn the label distribution of facial affects. For the two mainly used graph representations, hand-crafted features (e.g., *LBP* [69], *Gabor* [59], *HOG* [55], [74]) or deep-based features (e.g., *VGG* [78], *ResNet* [85]) are employed to enhance the node representation similar to many non-graph FER methods [99], [110]. For reasoning approaches, early studies prefer to capture the relations of individual node from predefined graph structures using tracking strategies [26], [64], [70], [77] or traditional machine learning models (e.g., *RF* [58], *BRNN* [59], *CNN* [55]). In some of the latest work, *GCNs* become one of the mainstream choice and shows the state-of-the-art performances on both posed and in-the-wild databases. Another observation is that the framework of combining the spatio-temporal graph representation combined and *GNNs* is getting more attention in FER studies [74], [75], [78].

Despite many graph-based studies have showed improvements in predicting facial affects, there are still some potential topics for FER. One thing is that the goal of existing methods stays on classifying basic facial affects. No study of using graph-based methods to recognize compound affects (or mixture affects), whose labels are provided by recent databases like RAF-DB and EmotioNet, is reported. One

TABLE 2
Performance summary of representative graph-based FER methods discussed in this Paper

References 'year	Prep. ¹		Representation ²			Reasoning ³		Posed Database ⁴	Wild Database	Validation ⁵
	B.B.	LM	Cat.	Node	Edge	Model	Classif.			
Kotsia <i>et al.</i> [64] '07	○	104	$S : \mathcal{L}$	\mathbb{C}	Δ	---	SVM	CK <i>ar</i> : 99.7%	/	LO CV
Zafeiriou <i>et al.</i> [70] '08	●	/	$S : \mathcal{P}$	NM	L	---	EGM	CK <i>ar</i> : 97.1%	/	LO CV
Tanchotsrinon <i>et al.</i> [50] '11	●	14	$S : \mathcal{L}$	\mathbb{C}	$M+\mathbb{E}$	/	MLP	CK <i>ar</i> : 95.24%	/	HO
Mohseni <i>et al.</i> [26] '14	○	50	$S : \mathcal{L}$	\mathbb{C}	$M+\mathbb{E}$	---	Adabst	MMI <i>ar</i> : 87.7%	/	10F CV
Rivera <i>et al.</i> [77] '15	●	/	$ST : \mathcal{R}$	Histo.	DNG	---	SVM	CK+ <i>ar</i> : 100%; MMI <i>ar</i> : 97.6%; Oulu <i>ar</i> : 98.4%	/	10F CV
Yao <i>et al.</i> [69] '15	●	/	$S : \mathcal{R}$	LBP	L	/	SVM/CNN	/	SFEW <i>ar</i> : 55.38%; AFEW <i>ar</i> : 53.80%;	HO
Durmuşoğlu <i>et al.</i> [51] '16	●	18	$S : \mathcal{L}$	\mathbb{C}	$F+\mathbb{E}$	CFS	MLP	MUG [152]: <i>ar</i> : 91.22%	/	HO
Dapogny <i>et al.</i> [58] '18	●	49	$S : \mathcal{L}$	$\mathbb{C}+\text{HOG}$	Δ	AE	RF	CK+ <i>ar</i> : 93.4%; BU-4DFE <i>ar</i> : 75.0%	SFEW <i>ar</i> : 37.1%	10F-SI CV, HO
Zhong <i>et al.</i> [59] '19	●	46	$S : \mathcal{L}$	Gabor	$F+\mathbb{E}$	BRNN	SoftMax	CK+ <i>ar</i> : 98.27%; MMI <i>ar</i> : 94.44%; Oulu <i>ar</i> : 93.06%	/	10F-SI CV
Wu <i>et al.</i> [71] '19	●	/	$S : \mathcal{P}$	Pixel	\mathbb{E}	GCN	SoftMax	CK+ <i>ar</i> : 99.78%; JAFEE [153]: <i>ar</i> : 94.44%	/	HO
Chen <i>et al.</i> [91] '20	●	/	$AU : \mathcal{O}$	Φ	KNN	/	SoftMax	CK+ <i>ar</i> : 93.08%; MMI <i>ar</i> : 70.49%; Oulu <i>ar</i> : 63.85%	SFEW <i>ar</i> : 56.50%; RAF <i>ar</i> : 85.53%; AffNet <i>ar</i> : 59.35%	CD
Liu <i>et al.</i> [55] '20	●	68	$S : \mathcal{L}$	$\mathbb{C}+\text{HOG}$	Δ	CNN	SoftMax	CK+ <i>ar</i> : 97.67%; MMI <i>ar</i> : 80.11%	SFEW <i>ar</i> : 55.36%	10F-SI CV, HO
Xie <i>et al.</i> [73] '20	●	/	$S : \mathcal{P}$	ResNet	K-means	GCN	SoftMax	CK+ <i>ar</i> : 85.27%; JAFEE <i>ar</i> : 61.50%	SFEW <i>ar</i> : 56.43%; FER2013 <i>ar</i> : 58.95%; ExpW <i>ar</i> : 68.50%	CD
Zhou <i>et al.</i> [74] '20	●	34	$ST : \mathcal{L}$	$\mathbb{C}+\text{HOG}$	$M+\mathbb{H}$	GCN	SoftMax	CK+ <i>ar</i> : 98.63%; Oulu <i>ar</i> : 87.23%	/	10F-SI CV
Hassan <i>et al.</i> [57] '20	○	20	$S : \mathcal{L}$	\mathbb{C}	$F+\mathbb{E}$	$gSpan$	MLP	CK+ <i>ar</i> : 98.63%; Oulu <i>ar</i> : 87.23%	/	HO
Liu <i>et al.</i> [78] '20	●	/	$ST : \mathcal{F}$	VGG	F	GCN	BiLSTM	CK+ <i>ar</i> : 99.54%; Oulu <i>ar</i> : 91.04%; MMI <i>ar</i> : 85.89%	/	10F-SI CV
Zhou <i>et al.</i> [75] '20	●	44	$ST : \mathcal{L}$	$\mathbb{C}+\text{HOG}$	$L+\mathbb{H}$	GCN	SoftMax	CK+ <i>ar</i> : 98.92%; Oulu <i>ar</i> : 87.50%	AFEW <i>ar</i> : 45.12%	10F-SI CV, HO

¹ Prep.: processing; B.B.: bounding boxes; ● = Yes, ○ = No; LM: landmarks.

² Cat.: category; $S/ST/AU$: {spatial; spatio-temporal; AU-level} representation; $: \mathcal{L}/\mathcal{R}/\mathcal{P}/\mathcal{O}/\mathcal{F}$: {landmark; region; patch; other; frame}-level graph; \mathbb{C} : landmark coordinates; Histo.: histograms; Φ : label distributions; Δ : triangulation; $L/M/F$: {learning; manual; full} connections; \mathbb{E} : Euclidean distance; \mathbb{H} : Hop distance.

³ Classif.: classifier; ---: tracking; $gSpan$: graph mining.

⁴ *ar*: average accuracy rate.

⁵ CV: cross validation; LO: leave-one-out; HO: holdout validation; 10F: 10-folds; SI: subject independent; CD: cross database validation.

possible resolution is to introduce AU-level graph representations that can describe fine-grained macro expressions with closer inter-class distances. The other topic is effective graph-based representation due to the big gap between the performance of current methods and the acceptable result in practice when analyzing in-the-wild facial affects. In addition, since existing databases lack sufficient dynamic annotated samples, the evaluation of newly spatio-temporal graphs in large-scale conditions remains to be explored.

6.2 Action Unit Detection

The AU detection (AUD) facilitates a comprehensive analysis of the facial affect and is typically formulated as a multi-task problem that learns a two-class classification model for

each AU. It can not only expand the recognition categories of macro-expressions through the AU combination [54], but also can be used as a pre-step to enhance the recognition of micro-expressions [87]. Comparing with graph-based FER, the widely using of graph structures has a longer history in AU detection [28] and has played a more dominant role. Table 3 presents a summary of graph-based AU detection methods including the performance comparison.

Specifically, the spatial graph and the AU-level graph are equally popular in the representation part of AUD. An interesting observation is that, no matter landmark-level or region-level, all the spatial graphs constructed in the listed AUD methods employed facial landmarks [54], [55], [58], [60], [65], [66], [67]. The possible reason is that the

TABLE 3
Performance summary of representative graph-based AUD methods discussed in this Paper

References 'year	Prep. ¹		Representation ²			Reasoning ³		Database ⁴	Validation ⁵
	B.B.	LM	Cat.	Node	Edge	Model	Output		
Tong <i>et al.</i> [79] '07	•	/	$\mathcal{AU} : \mathcal{B}$	<i>Gabor</i>	Φ	<i>DBN</i>	<i>Adabst</i>	CK <i>ar</i> : 99.33%; MMI (CK) <i>ar</i> : 93.9%	LOSO CV, CD
Zhu <i>et al.</i> [80] '14	•	49	$\mathcal{AU} : \mathcal{B}$	$\mathbb{C} + \textit{Gabor}$	Φ	<i>DBN</i>	<i>MPE</i>	CK+ <i>ar</i> : 90.48%, f_1 : 0.7072; DISFA <i>ar</i> : 93.56%, f_1 : 0.7095	2F, 10F CV
Kaltwang <i>et al.</i> [54] '15	◦	66	$\mathcal{S} : \mathcal{L}$	\mathbb{C}	\mathcal{L}	$\mathcal{L}\mathcal{T}$		DISFA <i>corr</i> : 0.43, <i>mse</i> : 0.39, <i>icc</i> : 0.36	9F CV
Sechkova <i>et al.</i> [60] '16	◦	49	$\mathcal{S} : \mathcal{L}$	$\mathbb{C} + \textit{SIFT}$	\mathcal{L}	<i>Graph Emb.</i>	<i>SVM</i>	CK+ <i>ar</i> : 92.7%	LOSO CV
Walecki <i>et al.</i> [88] '17	◦	/	$\mathcal{AU} : \mathcal{M}$	<i>CNN</i>	\mathcal{L}	<i>CRF</i>	<i>Ordi. Regr.</i>	FERA2015 [19] <i>icc</i> : 0.63, <i>mae</i> : 1.23; DISFA <i>icc</i> : 0.45, <i>mae</i> : 0.61	HO
Corneanu <i>et al.</i> [84] '18	•	/	$\mathcal{AU} : \mathcal{M}$	<i>VGG</i>	Φ	<i>RNN</i>	<i>Sigmoid</i>	BP4D f_1 : 61.7%; DISFA f_1 : 56.7%	3F-SI CV
Dapogny <i>et al.</i> [58] '18	•	49	$\mathcal{S} : \mathcal{L}$	$\mathbb{C} + \textit{HOG}$	Δ	<i>AE</i>	<i>RF</i>	CK+ <i>auc</i> : 95.3%, f_1 : 78.8%, nf_1 : 86.5%; BP4D: <i>auc</i> : 72.7%, f_1 : 55.7%, nf_1 : 63.6%; DISFA <i>auc</i> : 82.4%, f_1 : 49.1%	10F-SI CV
Li <i>et al.</i> [83] '19	•	20	$\mathcal{AU} : \mathcal{M}$	$\mathbb{C} + \textit{VGG}$	$\mathcal{M} + \mathcal{L}$	<i>GGNN</i>	<i>FCN</i>	BP4D <i>auc</i> : 74.1%, f_1 : 62.9%; DISFA <i>auc</i> : 80.7%, f_1 : 55.9%	no report
Niu <i>et al.</i> [90] '19	•	/	$\mathcal{AU} : \mathcal{O}$	\mathbb{W}	<i>Trans. K</i>	<i>GCN</i>	<i>FCN</i>	BP4D f_1 : 59.8%; EmotionNet f_1 : 68.1%	3F-SI CV, HO
Liu <i>et al.</i> [67] '20	•	19	$\mathcal{S} : \mathcal{R}$	<i>EAC-Net + AE</i>	\mathcal{M}	<i>GCN</i>	<i>FCN</i>	BP4D <i>auc</i> : 87.3%, f_1 : 62.8%; DISFA <i>auc</i> : 74.6%, f_1 : 55.0%	3F-SI CV
Fan <i>et al.</i> [66] '20	•	20	$\mathcal{S} : \mathcal{R}$	<i>ResNet</i>	$\mathbb{KNN} + \mathbb{E}$	<i>DG-CNN</i>	<i>Htm. Regr.</i>	BP4D <i>icc</i> : 0.72, <i>mae</i> : 0.58; DISFA <i>icc</i> : 0.47, <i>mae</i> : 0.20	3F-SI CV
Liu <i>et al.</i> [55] '20	•	68	$\mathcal{S} : \mathcal{L}$	$\mathbb{C} + \textit{HOG}$	Δ	<i>CNN</i>	<i>FCN</i>	CK+ <i>auc</i> : 92.9%	10F-SI CV
Zhang <i>et al.</i> [65] '20	•	18	$\mathcal{S} : \mathcal{R}$	<i>HRNetV2</i>	\mathcal{L}	<i>GCN</i>	<i>Htm. Regr.</i>	BP4D f_1 : 63.5%; DISFA f_1 : 62.0%	3F-SI CV
Zhou <i>et al.</i> [87] '20	•	/	$\mathcal{AU} : \mathcal{M}$	<i>Optical-flow + Inception</i>	\mathcal{L}	<i>GCN</i>	<i>Softmax</i>	CASME II (SAMM) f_1 : 61.10%; SAMM (CASME II) f_1 : 57.22%	LOSO CV, CD
Cui <i>et al.</i> [82] '20	◦	51	$\mathcal{AU} : \mathcal{B}$	<i>LBP</i>	Φ	<i>DBN</i>	<i>LR/ CNN/ SVM</i>	CK+ f_1 : 0.830; BP4D f_1 : 0.687; EmotionNet f_1 : 0.626; MMI (CK+) f_1 : 0.532	5F-SI CV, CD
Song <i>et al.</i> [89] '21	•	/	$\mathcal{AU} : \mathcal{M}$	<i>ResNet</i>	<i>Rand. M</i>	<i>GAT</i>	<i>Softmax</i>	BP4D <i>ar</i> : 78.2%, f_1 : 63.3%; DISFA <i>ar</i> : 93.4%, f_1 : 60.0%	3F-SI CV

¹ Prep.: processing; B.B.: bounding boxes; • = Yes, ◦ = No; LM: landmarks.

² Cat.: category; \mathcal{S}/\mathcal{AU} : {spatial; AU-level} representation; $\mathcal{L}/\mathcal{R}/\mathcal{B}/\mathcal{M}$: {landmark; region; label; map}-level graph; \mathbb{C} : landmark coordinates; Φ : label distributions; Δ : triangulation; \mathcal{L}/\mathcal{M} : {learning; manual} connections; \mathbb{E} : Euclidean distance; *Trans. K*: transfer knowledge; *Rand. M*: random mask.

³ *Graph Emb.*: graph embedding; *Ordi. Regr.*: ordinal regression; *Htm. Regr.*: heatmap regression.

⁴ *ar*: average accuracy rate; f_1 : F1 score; nf_1 : F1-norm score; *corr*: Pearson correlation coefficient; *mae*: mean absolute error; *mes*: mean squared error; *icc*: intra-class correlation coefficient, ICC(3,1); *auc*: area under the receiver operating characteristic curve; DB1 (DB2): train on DB2, test on DB1.

⁵ CV: cross validation; LOSO: leave-one-subject-out; (K)F: k-folds; SI: subject independent; HO: holdout validation; CD: cross database validation.

landmark information is helpful and effective for locating the facial areas where AUs may occur. In this setting, their node representations are close to that in spatial graphs of FER methods, which usually combine geometric coordinates with appearance features (e.g., *SIFT* [60], *HOG* [55], [58]). Although some AUD methods using AU-level graphs also exploited traditional (e.g., *Gabor* [79], [80], *LBP* [82]) or deep features (e.g., *VGG* [84]) to introduce appearance information, their graph representations were basically initialized from the AU label distribution of the training set. This has led to the *DBN* model becoming a major approach in the relational reasoning stage [79], [80], [82]. Another similar trend to graph-based FER is that *GNNs* have been widely utilized to learn the latent dependency among individual AUs in recent studies, such as *GCN* [65], [67], [87], [90], *GAT* [89], *GGNN* [83] and *DG-CNN* [66]. But the difference is that the *FCN* [55], [67], [83], [90] or regression models [65], [66],

[88] are often applied for predicting labels instead of *Softmax* classifier [87], [89].

A special line of AUD research analyzes the facial affects by estimating the AU intensities, which could have greater information value in understanding complex affective states [154]. Even though a few attempts in estimating AU intensities based on graph structures have existed [54], [66], [84], the study of using the latest spatio-temporal graph representations and *GNNs* has not been reported. Another big challenge in AUD is insufficient and imbalanced samples. The recent graph-based methods using transfer knowledge [82], [90] or uncertainty learning [89] were proposed to address this problem. They showed an advantage of graph-based method in this topic and are helpful to implement AUD in large-scale unlabeled data.

TABLE 4
Performance summary of representative graph-based MER methods discussed in this Paper

References 'year	Prep. ¹		Representation ²			Reasoning ³		Database ⁴	Validation ⁵
	B.B.	LM	Cat.	Node	Edge	Model	Classif.		
Liu <i>et al.</i> [68] '18	•	66	$S : \mathcal{R}$	<i>Optical-flow</i>	<i>KNN</i>	<i>GraphSC</i>	<i>SVM</i>	SMIC <i>ar</i> : 70.51%, f_1 : 70.41%; CASME [155] <i>ar</i> : 74.83%, f_1 : 74.95%; CASME II <i>ar</i> : 66.95%, f_1 : 69.11%	LOSO CV
Lo <i>et al.</i> [81] '20	•	/	$\mathcal{AU} : \mathcal{B}$	Φ	<i>KNN</i>	<i>GCN</i>	<i>Softmax</i>	CASME II (7 cl.) <i>ar</i> : 42.71%	LOSO CV
Lei <i>et al.</i> [62] '20	•	28	$S : \mathcal{L}$	<i>TCN</i>	<i>F</i>	<i>G-TCN</i>	<i>Softmax</i>	CASME II <i>ar</i> : 73.98%, f_1 : 72.46%; SAMM (5 cl.) <i>ar</i> : 75.00%, f_1 : 69.85%; SAMM (4 cl.) <i>ar</i> : 80.50%, f_1 : 76.57%	LOSO CV
Xie <i>et al.</i> [85] '20	•	/	$\mathcal{AU} : \mathcal{M}$	<i>3DCNN</i>	<i>L</i>	<i>GCN</i>	<i>Softmax</i>	CASME II <i>ar</i> : 0.712, f_1 : 0.355; CASME II (7 cl.) <i>ar</i> : 0.561, f_1 : 0.394; SAMM (3 cl.) <i>ar</i> : 0.702, f_1 : 0.433; SAMM <i>ar</i> : 0.523, f_1 : 0.357 SMIC (CASME II): <i>ar</i> : 0.344, f_1 : 0.319; SMIC (SAMM): <i>ar</i> : 0.451, f_1 : 0.309	LOSO CV, CD
Buhari <i>et al.</i> [53] '20	•	68	$S : \mathcal{L}$	\mathbb{C}	$F+\mathbb{E}+\mathbb{G}$	/	<i>SVM</i>	SMIC <i>ar</i> : 76.67%, f_1 : 0.75; CASME II <i>ar</i> : 75.04%, f_1 : 0.74; CAS(ME) ² <i>ar</i> : 81.85%, f_1 : 0.80; SAMM <i>ar</i> : 87.33%, f_1 : 0.87	LOSO CV
Zhou <i>et al.</i> [87] '20	•	/	$\mathcal{AU} : \mathcal{M}$	<i>Optical-flow</i> <i>+Inception</i>	<i>L</i>	<i>GCN</i>	<i>Softmax</i>	CASME II (SAMM) <i>war</i> : 0.708, <i>uar</i> : 0.595; SAMM (CASME II) <i>war</i> : 0.662, <i>uar</i> : 0.588; CASME II+SAMM f_1 : 0.685, wf_1 : 0.742)	LOSO CV, CD

¹ Prep.: processing; B.B.: bounding boxes; • = Yes, ○ = No; LM: landmarks.

² Cat.: category; S/\mathcal{AU} : {spatial; AU-level} representation; $\mathcal{L}/\mathcal{B}/\mathcal{M}$: {landmark; label; map}-level graph; \mathbb{C} : landmark coordinates; Φ : label distributions; L/F : {learning; fully} connections; \mathbb{E} : Euclidean distance; \mathbb{G} : Gradient using slope equation.

³ Classif.: classifier; *GraphSC*: graph sparse coding; *G-TCN*: graph TCN.

⁴ *ar*: average accuracy rate; f_1 : F1 score; *war*: weighted average recall; *wf_1*: weighted F1 score; *uar*: unweighted average recall; (N) cl.: (N) affective classes; DB1 (DB2): train on DB2, test on DB1.

⁵ CV: cross validation; LOSO: leave-one-subject-out; CD: cross database validation.

6.3 Micro-Expression Recognition

Micro-expressions are fleeting and involuntary facial affects that people usually have in high stake situations when attempt to conceal or mask their true feelings. The earliest well-known studies came from Haggard and Isaacs [156] as well as Ekman and Friesen [157]. Generally, a micro-expression only lasts 1/25 to 1/2 second long and is too subtle and fleeting for an untrained people to perceive. Therefore, developing an automatic micro-expression recognition (MER) system is valuable in reading human hidden affective states. Besides the short duration, the characteristics of low intensity and localization make it challenging to analyze micro-expressions using computer vision and machine learning methods.

To this end, graph-based MER methods have been designed to address the above challenges, and have become appealing in the past two years [68], especially in 2020 [53], [62], [81], [85], [87]. Table 4 lists the reported performance of a few representative recent work of graph-based MER. In terms of representation types, these methods fall into the landmark-level spatial graph [53], [62], [68] and the AU-level graph [81], [85], [87]. For the former, their idea is to use landmarks to locate and analyze specific facial areas to deal with the local response and the subtleness of micro-expressions. And for the latter, they aim to infer the AU relationship to improve the final performance. The difference in processing ideas is also reflected in the reasoning procedure. Approaches like *GraphSC* [68] and variant *CNN* [62] are exploited in the landmark-level graph to integrate

the individual node feature representations. While the *GCN* is employed to learn an optimal graph structure of the AU dependency knowledge from training data and make predictions. But one common thing is that almost all the methods except [53] consider the local appearance in a spatio-temporal way by using *optical-flow* or *3DCNN*.

A problem in the graph-based micro-expression analysis is the lack of large-scale in-the-wild databases. The small sample size limits the AU-level graph representation that rely on initializing the AU relationship from the AU label distribution of the training set. And the lab-controlled data make it difficult to follow the trend in FER studies, which generalizes the graph-based FAA methods in real-world scenarios. However, the analysis of uncontrolled micro-expressions is very important, because micro-expressions can occur with macro-expressions simultaneously in many real cases. For example, furrowing on the forehead slightly and quickly when smiling indicates the true feeling of a person [157]. For another thing, since the evolutionary appearance information is crucial for the micro-expression analysis, building a spatio-temporal graph representation that can model the duration and dynamic of micro-expressions is also a helpful but unexplored topic.

6.4 Special Tasks

The graph-based methods also play an important role in several special FAA tasks, such as pain detection [54], non-basic emotion recognition [72], multi-modal emotion recognition [76], [92] and emotion tagging [93]. Table 5 lists a

TABLE 5
Performance summary of special graph-based FAA methods discussed in this Paper

References 'year	Prep. ¹		Representation ²			Reasoning		Database ³	Validation ⁴
	B.B.	LM	Cat.	Node	Edge	Model	Output		
Kaltwang <i>et al.</i> [54] '15	◦	66	$S : \mathcal{L}$	\mathbb{C}	L	LT		ShoulderPain [158] <i>corr</i> : 0.23, <i>mse</i> : 0.60	8F CV
Zhang <i>et al.</i> [72] '19	•	/	$S : \mathcal{P}$	VGG	L	GCN	Softmax FCN	EMOTIC (26 cl.) <i>prc</i> : 28.42%; EMOTIC (VAD) <i>er</i> : 0.9	HO
Chen <i>et al.</i> [76] '19	•	68	$ST : \mathcal{L}$	\mathbb{C}	$\Delta+M$	GCN	FCN	CES [23] <i>val_ccc</i> : 0.515, <i>aro_ccc</i> : 0.513	HO
Chien <i>et al.</i> [92] '20	◦	/	\mathcal{O}	3DCNN	<i>Trans. K</i>	GCN	FCN	Amigos [159] (Ascertain [160]) <i>val_uar</i> : 0.798, <i>aro_uar</i> : 0.679; Ascertain (Amigos) <i>val_uar</i> : 0.704, <i>aro_uar</i> : 0.569	CD
Xu <i>et al.</i> [93] '20	◦	/	\mathcal{O}	AE	Φ	GCN	GAN	NVIE [161] <i>ar</i> : 0.5632, f_1 : 0.6573, <i>mif</i> ₁ : 0.6614, <i>maf</i> ₁ : 0.6412; FilmStim [162] <i>ar</i> : 0.4669, f_1 : 0.5782, <i>mif</i> ₁ : 0.6131, <i>maf</i> ₁ : 0.5931	HO

¹ Prep.: processing; B.B.: bounding boxes; • = Yes, ◦ = No; LM: landmarks.

² Cat.: category; $S/ST/O$: {spatial; spatio-temporal; other} representation; \mathcal{L}/\mathcal{P} : {landmark; patch}-level graph; \mathbb{C} : landmark coordinates; Φ : label distributions; Δ : triangulation; M/L : {manual/learning} connections; *Trans. K*: transfer knowledge.

³ *corr*: Pearson correlation coefficient; *mes*: mean squared error; *prc*: area under the precision recall curves; *er*: average error rate; *val/aro*: valance/arousal; *ccc*: concordance correlation coefficient; *uar*: unweighted average recall; (N) cl.: (N) affective classes; VAD: valence, arousal, dominance; DB1 (DB2): train on DB2, test on DB1; *ar*: average accuracy rate; f_1 : F1 score; *mif*₁: micro F1 score; *maf*₁: macro F1 score.

⁴ HO: holdout validation; CD: cross database validation.

summary of the latest graph-based FAA methods for special tasks.

For graph constructions including two special graphs [92], [93], the strategies of their node representations and edge initialization are similar to that in graph-based FER, MER and AUD methods. While for the reasoning step, GCN is the accepted option. This observation implies that the framework of the graph-based method discussed in this paper can be easily extended to many other FAA tasks and promote performance improvement.

7 CONCLUSION

In this survey, we expounded graph-based facial affect analysis methods by dissecting into fundamental components, and we discussed their potential and limitations. To summarize, we provide an overall discussion and highlight open directions.

7.1 Discussion

In this paper, we have focused on giving a general review into the appealing field of the graph-based FAA. We have started by introducing the fundamental preprocessing steps. An in-depth discussion about two major aspects have been followed, including the different kinds of graph-based affective representations and their corresponding relational reasoning models. Then, we have presented commonly used public databases. The representative recent studies have been summarized in terms of macro- and micro-expression recognition, action unit detection and other special FAA applications.

7.1.1 Representation

When encoding facial affect into graph representations, strategies vary according to both node element and timing. Specifically, the spatial graph regards an affective face as multiple local crucial facial areas and model the relationship

among them, while the spatio-temporal graph also considers the temporal evolution in continuous frames. Another distinctive representation is the AU-level graph. Since each AU and its co-occurrence dependency provide certain semantics of facial affects, most of the AU-level graphs are built by learning a distribution from existing available data. Other representations like multi-modal graphs employ the graph structure as a bridge to establish the information interaction from different modality.

There are various techniques for generating node attributes and initializing edge connections. The appearance and geometric information can be separately or jointly extracted by either pre-defined descriptors or deep models for each node, while the edge links can be obtained through manual linking, automatic learning or calculation rules. Regardless of these approaches, the node attribute generation and the edge connection initialization are followed by most methods. For instance, spatial graphs and AU-level graphs are slightly different depending on the node element, but they can share the similar node attributes (e.g., landmark coordinates [55], [83]) or edge connections (e.g., KNN [66], [91]). For the timing, some methods also exploited the dynamic information in the representation stage [68], [85], [87], even though they did not construct a whole space-time representation like spatio-temporal graphs.

7.1.2 Relational reasoning

Relational reasoning approaches infer latent relationships or inherent dependencies of graph nodes in terms of space, time, semantic, etc. The category of front graph representation will affect the technique choice of relational reasoning to a certain extent. Both traditional and advanced machine learning methods have been proposed to conduct the relational reasoning on affective graphs. DBNs explicitly update the relevant graph structure along with other pre-extracted local features and have been mostly used for AU-label representations. For deep learning methods, standard models

can execute transformation of input format or adjustment of network architecture to meet the requirements of processing graph relational reasoning, while GNNs deal with structured graph data based on their specially designed architecture. The two types of deep models can contribute to FAA either independently or cooperatively and are versatile for a variety of graph representations. Other basic machine learning methods, including graph structure learning and graph feature selection, have also been provided for relational reasoning, which have become less popular due to applicability and performance limitations.

7.2 Open Direction

Despite significant advances, the graph-based FAA is still an appealing field that has many open directions.

7.2.1 In-the-wild scenarios

Although many efforts have been done to perform graph-based FAA in naturalistic conditions [55], [58], [69], [75], [82], [85], [90], [91], even the state-of-the-art performance is far from actual applications. Factors like illumination, head pose and part occlusion are challenging in constructing an effective graph representation. For one thing, large illumination changes and head pose variations will impair the accuracy of face detection and registration, which is vital for establishing landmark-level graphs. The graph representation without landmarks [69], [73] should be a possible direction to avoid this problem. For another thing, missing face parts resulted by camera view or context occlusion make it difficult to encode enough facial information and obtain meaningful connections in an affective graph. Pioneer work [58], [75] tried to exploit a sub-graph without masked facial parts or generate adaptive edge links to alleviate the influence. Unfortunately, there was still a big performance decrease compared to that in normal conditions. Therefore, more effective graph representation should be proposed to account for these problems.

7.2.2 3D and 4D facial affects

Using 3D and 4D face images might be another reasonable topic because the 3D face shape provides additional depth information and contains subtle facial deformations in a dynamic way, so that they are intuitively insensitive to pose and light changes. Some studies transformed the 3D face to 2D images and generated graph representations [58], [66], [83], [84], but they have not fully taken the advantage of the 3D data. Alternatively, attempts of both non-graph-based [163] and graph-based methods [63] have been explored to directly conduct FAA on 3D or 4D faces. Since the structure of 3D face mesh is naturally close to the graph structure, employing the graph representation and reasoning to handle 3D face images will promote the improvement of in-the-wild FAA. Besides, there is also a potential topic of using 3D and 4D data with graph-based method in micro-expression recognition.

7.2.3 Valence and arousal

Estimating the continuous dimension is a rising topic in FAA. Not like discrete labels, the valence indicates the positive or negative characteristic of a facial affect, while the

arousal denotes the intensity level of the activation about a facial affect. In recent years, some related competitions have been held at CVPR 2017 [21], BMVC 2019 [164] and FG 2020 [165]. And large-scale FAA databases (Aff-Wild I [21], II [165]) containing valence-arousal (V-A) annotations have been released to support the continuous analysis of facial affects. Several graph-based method have been proposed to perform the V-A measurement [54], [66], [88]. However, these methods have only been evaluated on lab-controlled databases, their performances on in-the-wild databases have not been reported.

7.2.4 Context and multi-modality

Most current FAA methods only consider a single face in one image or one sequence. But in real cases, people usually have affective behaviors including facial expression, body gesture and emotional speaking [166]. And these facial affective displays are highly associated to context surroundings that include but not limited to the affective behavior of another people in social interactions or inanimate objects. Existing studies like [72] and [73] employed the graph reasoning to infer the relationship between target face and other objects in the same image for enhanced FAA. Future graph-based studies should combine facial affects with other helpful context information and perform the analysis on a fuller scope. Another reasonable topic is to introduce additional data channels that is multi-modality. The graph-based methods have also successfully extended to process multi-modal affect analysis tasks with information such as audio [76] and physiological signal [92], which shows a good research prospect.

7.2.5 Cross-database and transfer learning

Insufficient annotations and imbalanced labels are two problems that limits the development of FAA research. One possible resolution is to use the graph-based transfer learning. Efforts like [82], [89], [90] exploited the graph structure to solve this challenge in terms of semi-supervision, label correction and generation, and uncertainty measurement respectively. On the other hand, the performance of affective features extracted by using graph-based representation and reasoning has been proved through cross-database validation in all macro-expression recognition [73], [91] and micro-expression recognition [85], [87] and AU detection [79], [82], [87]. This reveals that the graph-based method is valuable in improving the generalization of affective features.

ACKNOWLEDGMENTS

Funding: This work was supported by the China Scholarship Council [CSC, No.202006150091].

The authors would like to thank Muzammil Behzad and Tuomas Varanka for providing materials and suggestions of the Figures used in this paper.

REFERENCES

- [1] C. Darwin and P. Prodger, *The expression of the emotions in man and animals*. Oxford University Press, USA, 1998.
- [2] M. S. Gazzaniga, R. B. Ivry, and G. Mangun, *Cognitive Neuroscience. The biology of the mind*, (2014). Norton: New York, 2006.

- [3] R. W. Picard, E. Vyzas, and J. Healey, "Toward machine emotional intelligence: Analysis of affective physiological state," *IEEE transactions on pattern analysis and machine intelligence*, vol. 23, no. 10, pp. 1175–1191, 2001.
- [4] E. Sariyanidi, H. Gunes, and A. Cavallaro, "Automatic analysis of facial affect: A survey of registration, representation, and recognition," *IEEE transactions on pattern analysis and machine intelligence*, vol. 37, no. 6, pp. 1113–1133, 2014.
- [5] R. E. Jack, O. G. Garrod, H. Yu, R. Caldara, and P. G. Schyns, "Facial expressions of emotion are not culturally universal," *Proceedings of the National Academy of Sciences*, vol. 109, no. 19, pp. 7241–7244, 2012.
- [6] M. G. Calvo, A. Gutiérrez-García, and M. Del Líbano, "What makes a smiling face look happy? visual saliency, distinctiveness, and affect," *Psychological research*, vol. 82, no. 2, pp. 296–309, 2018.
- [7] P. Rodriguez, G. Cucurull, J. González, J. M. Gonfaus, K. Nasrollahi, T. B. Moeslund, and F. X. Roca, "Deep pain: Exploiting long short-term memory networks for facial expression classification," *IEEE transactions on cybernetics*, pp. 1–11, 2017. [Online]. Available: <https://doi.org/10.1109/TCYB.2017.2662199>
- [8] S. D'Mello, R. W. Picard, and A. Graesser, "Toward an affect-sensitive autotutor," *IEEE Intelligent Systems*, vol. 22, no. 4, pp. 53–61, 2007.
- [9] J. Lou, Y. Wang, C. Nduka, M. Hamed, I. Mavridou, F.-Y. Wang, and H. Yu, "Realistic facial expression reconstruction for vr hmd users," *IEEE Transactions on Multimedia*, vol. 22, no. 3, pp. 730–743, 2019.
- [10] P. Ekman and W. V. Friesen, "Constants across cultures in the face and emotion," *Journal of personality and social psychology*, vol. 17, no. 2, pp. 124–129, 1971.
- [11] P. Ekman, "Strong evidence for universals in facial expressions: a reply to russell's mistaken critique," *Psychological Bulletin*, vol. 115, no. 2, pp. 268–287, 1994.
- [12] E. Friesen and P. Ekman, "Facial action coding system: a technique for the measurement of facial movement," *Palo Alto*, vol. 3, no. 2, p. 5, 1978.
- [13] P. Ekman, "Facial action coding system (facs)," *A human face*, 2002.
- [14] R. Plutchik, "A general psychoevolutionary theory of emotion," in *Theories of emotion*. Elsevier, 1980, pp. 3–33.
- [15] M. K. Greenwald, E. W. Cook, and P. J. Lang, "Affective judgment and psychophysiological response: dimensional covariation in the evaluation of pictorial stimuli," *Journal of psychophysiology*, vol. 3, no. 1, pp. 51–64, 1989.
- [16] J. A. Russell, "Evidence of convergent validity on the dimensions of affect," *Journal of personality and social psychology*, vol. 36, no. 10, p. 1152, 1978.
- [17] L. Yin, X. Chen, Y. Sun, T. Worm, and M. Reale, "A high-resolution 3d dynamic facial expression database," in *2008 8th IEEE International Conference on Automatic Face and Gesture Recognition*, 2008, pp. 1–6.
- [18] M. F. Valstar, B. Jiang, M. Mehu, M. Pantic, and K. Scherer, "The first facial expression recognition and analysis challenge," in *2011 IEEE International Conference on Automatic Face Gesture Recognition (FG)*. IEEE, 2011, pp. 921–926.
- [19] M. F. Valstar, T. Almaev, J. M. Girard, G. McKeown, M. Mehu, L. Yin, M. Pantic, and J. F. Cohn, "Fera 2015-second facial expression recognition and analysis challenge," in *2015 11th IEEE International Conference and Workshops on Automatic Face and Gesture Recognition (FG)*, vol. 6. IEEE, 2015, pp. 1–8.
- [20] A. Dhall, G. Sharma, R. Goecke, and T. Gedeon, "Emotiw 2020: Driver gaze, group emotion, student engagement and physiological signal based challenges," in *Proceedings of the 2020 International Conference on Multimodal Interaction*, 2020, pp. 784–789.
- [21] S. Zafeiriou, D. Kollias, M. A. Nicolaou, A. Papaioannou, G. Zhao, and I. Kotsia, "Aff-wild: valence and arousal in-the-wild challenge," in *Proceedings of the IEEE conference on computer vision and pattern recognition workshops*, 2017, pp. 34–41.
- [22] C. F. Benitez-Quiroz, R. Srinivasan, Q. Feng, Y. Wang, and A. M. Martinez, "Emotionet challenge: Recognition of facial expressions of emotion in the wild," *arXiv preprint arXiv:1703.01210*, 2017. [Online]. Available: <https://arxiv.org/abs/1703.01210>
- [23] F. Ringeval, B. Schuller, M. Valstar, N. Cummins, R. Cowie, L. Tavabi, M. Schmitt, S. Alisamir, S. Amiriparian, E.-M. Messner et al., "Avec 2019 workshop and challenge: state-of-mind, detecting depression with ai, and cross-cultural affect recognition," in *Proceedings of the 9th International on Audio/Visual Emotion Challenge and Workshop*, 2019, pp. 3–12.
- [24] L. Stappen, A. Baird, G. Rizo, P. Tzirakis, X. Du, F. Hafner, L. Schumann, A. Mallol-Ragolta, B. W. Schuller, I. Lefter et al., "Muse 2020 challenge and workshop: Multimodal sentiment analysis, emotion-target engagement and trustworthiness detection in real-life media: Emotional car reviews in-the-wild," in *Proceedings of the 1st International on Multimodal Sentiment Analysis in Real-life Media Challenge and Workshop*, 2020, pp. 35–44.
- [25] D. L. Bimler and G. V. Paramei, "Facial-expression affective attributes and their configural correlates: components and categories," *Spanish Journal of Psychology*, vol. 9, no. 1, p. 19, 2006.
- [26] S. Mohseni, N. Zarei, and S. Ramazani, "Facial expression recognition using anatomy based facial graph," in *2014 IEEE International Conference on Systems, Man, and Cybernetics (SMC)*. IEEE, 2014, pp. 3715–3719.
- [27] C. A. Corneanu, M. O. Simón, J. F. Cohn, and S. E. Guerrero, "Survey on rgb, 3d, thermal, and multimodal approaches for facial expression recognition: History, trends, and affect-related applications," *IEEE transactions on pattern analysis and machine intelligence*, vol. 38, no. 8, pp. 1548–1568, 2016.
- [28] B. Martinez, M. F. Valstar, B. Jiang, and M. Pantic, "Automatic analysis of facial actions: A survey," *IEEE transactions on affective computing*, vol. 10, no. 3, pp. 325–347, 2017.
- [29] D. Kollias, P. Tzirakis, M. A. Nicolaou, A. Papaioannou, G. Zhao, B. Schuller, I. Kotsia, and S. Zafeiriou, "Deep affect prediction in-the-wild: Aff-wild database and challenge, deep architectures, and beyond," *International Journal of Computer Vision*, vol. 127, no. 6, pp. 907–929, 2019.
- [30] S. Li and W. Deng, "Deep facial expression recognition: A survey," *IEEE Transactions on Affective Computing*, 2020. [Online]. Available: <https://doi.org/10.1109/TAFFC.2020.2981446>
- [31] K. M. Goh, C. H. Ng, L. L. Lim, and U. U. Sheikh, "Micro-expression recognition: an updated review of current trends, challenges and solutions," *The Visual Computer*, vol. 36, no. 3, pp. 445–468, 2020.
- [32] L. Zhang, B. Verma, D. Tjondronegoro, and V. Chandran, "Facial expression analysis under partial occlusion: A survey," *ACM Computing Surveys (CSUR)*, vol. 51, no. 2, pp. 1–49, 2018.
- [33] X. Ben, Y. Ren, J. Zhang, S.-J. Wang, K. Kpalma, W. Meng, and Y.-J. Liu, "Video-based facial micro-expression analysis: A survey of datasets, features and algorithms," *IEEE Transactions on Pattern Analysis and Machine Intelligence*, 2021. [Online]. Available: <https://doi.org/10.1109/TPAMI.2021.3067464>
- [34] P. V. Rouast, M. Adam, and R. Chiong, "Deep learning for human affect recognition: Insights and new developments," *IEEE Transactions on Affective Computing*, 2019.
- [35] P. Viola and M. Jones, "Rapid object detection using a boosted cascade of simple features," in *Proceedings of the 2001 IEEE computer society conference on computer vision and pattern recognition. CVPR 2001*, vol. 1. IEEE, 2001, pp. 1–1.
- [36] K. Zhang, Z. Zhang, Z. Li, and Y. Qiao, "Joint face detection and alignment using multitask cascaded convolutional networks," *IEEE Signal Processing Letters*, vol. 23, no. 10, pp. 1499–1503, 2016.
- [37] Y. Xu, W. Yan, G. Yang, J. Luo, T. Li, and J. He, "Centerface: joint face detection and alignment using face as point," *Scientific Programming*, 2020. [Online]. Available: <https://doi.org/10.1155/2020/7845384>
- [38] I. Masi, Y. Wu, T. Hassner, and P. Natarajan, "Deep face recognition: A survey," in *2018 31st SIBGRAPI conference on graphics, patterns and images (SIBGRAPI)*. IEEE, 2018, pp. 471–478.
- [39] P. Lucey, J. F. Cohn, T. Kanade, J. Saraghi, Z. Ambadar, and I. Matthews, "The extended cohn-kanade dataset (ck+): A complete dataset for action unit and emotion-specified expression," in *2010 IEEE computer society conference on computer vision and pattern recognition-workshops*. IEEE, 2010, pp. 94–101.
- [40] A. Mollahosseini, D. Chan, and M. H. Mahoor, "Going deeper in facial expression recognition using deep neural networks," in *2016 IEEE Winter conference on applications of computer vision (WACV)*. IEEE, 2016, pp. 1–10.
- [41] P. Khorrami, T. Le Paine, K. Brady, C. Dagli, and T. S. Huang, "How deep neural networks can improve emotion recognition on video data," in *2016 IEEE international conference on image processing (ICIP)*. IEEE, 2016, pp. 619–623.
- [42] T. F. Cootes, G. J. Edwards, and C. J. Taylor, "Active appearance

- models," *IEEE Transactions on pattern analysis and machine intelligence*, vol. 23, no. 6, pp. 681–685, 2001.
- [43] X. Zhu and D. Ramanan, "Face detection, pose estimation, and landmark localization in the wild," in *2012 IEEE conference on computer vision and pattern recognition*. IEEE, 2012, pp. 2879–2886.
- [44] Z. Yu and C. Zhang, "Image based static facial expression recognition with multiple deep network learning," in *Proceedings of the 2015 ACM on international conference on multimodal interaction*, 2015, pp. 435–442.
- [45] R. Ranjan, V. M. Patel, and R. Chellappa, "Hyperface: A deep multi-task learning framework for face detection, landmark localization, pose estimation, and gender recognition," *IEEE transactions on pattern analysis and machine intelligence*, vol. 41, no. 1, pp. 121–135, 2017.
- [46] Z.-H. Feng, J. Kittler, M. Awais, P. Huber, and X.-J. Wu, "Face detection, bounding box aggregation and pose estimation for robust facial landmark localisation in the wild," in *Proceedings of the IEEE conference on computer vision and pattern recognition workshops*, 2017, pp. 160–169.
- [47] X. Dong, Y. Yang, S.-E. Wei, X. Weng, Y. Sheikh, and S.-I. Yu, "Supervision by registration and triangulation for landmark detection," *IEEE transactions on pattern analysis and machine intelligence*, 2020. [Online]. Available: <https://doi.org/10.1109/TPAMI.2020.2983935>
- [48] A. Bulat and G. Tzimiropoulos, "How far are we from solving the 2d & 3d face alignment problem?(and a dataset of 230,000 3d facial landmarks)," in *Proceedings of the IEEE International Conference on Computer Vision*, 2017, pp. 1021–1030.
- [49] N. Wang, X. Gao, D. Tao, H. Yang, and X. Li, "Facial feature point detection: A comprehensive survey," *Neurocomputing*, vol. 275, pp. 50–65, 2018.
- [50] C. Tanchotsrinon, S. Phimoltares, and S. Maneeroj, "Facial expression recognition using graph-based features and artificial neural networks," in *2011 IEEE International Conference on Imaging Systems and Techniques*. IEEE, 2011, pp. 331–334.
- [51] A. Durmuşoğlu and Y. Kahraman, "Facial expression recognition using geometric features," in *2016 International Conference on Systems, Signals and Image Processing (IWSSIP)*. IEEE, 2016, pp. 1–5.
- [52] M. Sabzevari, S. Toosizadeh, S. R. Quchani, and V. Abrishami, "A fast and accurate facial expression synthesis system for color face images using face graph and deep belief network," in *2010 International Conference on Electronics and Information Engineering*, vol. 2. IEEE, 2010, pp. V2–354.
- [53] A. M. Buhari, C.-P. Ooi, V. M. Baskaran, R. C. Phan, K. Wong, and W.-H. Tan, "Facs-based graph features for real-time micro-expression recognition," *Journal of Imaging*, vol. 6, no. 12, p. 130, 2020.
- [54] S. Kaltwang, S. Todorovic, and M. Pantic, "Latent trees for estimating intensity of facial action units," in *Proceedings of the IEEE Conference on Computer Vision and Pattern Recognition*, 2015, pp. 296–304.
- [55] Y. Liu, X. Zhang, Y. Lin, and H. Wang, "Facial expression recognition via deep action units graph network based on psychological mechanism," *IEEE Transactions on Cognitive and Developmental Systems*, vol. 12, no. 2, pp. 311–322, 2019.
- [56] P. Kakumanu and N. Bourbakis, "A local-global graph approach for facial expression recognition," in *2006 18th IEEE International Conference on Tools with Artificial Intelligence (ICTAI'06)*. IEEE, 2006, pp. 685–692.
- [57] A. K. Hassan and S. N. Mohammed, "A novel facial emotion recognition scheme based on graph mining," *Defence Technology*, vol. 16, no. 5, pp. 1062–1072, 2020.
- [58] A. Dapogny, K. Bailly, and S. Dubuisson, "Confidence-weighted local expression predictions for occlusion handling in expression recognition and action unit detection," *International Journal of Computer Vision*, vol. 126, no. 2, pp. 255–271, 2018.
- [59] L. Zhong, C. Bai, J. Li, T. Chen, S. Li, and Y. Liu, "A graph-structured representation with brnn for static-based facial expression recognition," in *2019 14th IEEE International Conference on Automatic Face & Gesture Recognition (FG 2019)*. IEEE, 2019, pp. 1–5.
- [60] T. Sechkova, K. Tonchev, and A. Manolova, "Action unit recognition in still images using graph-based feature selection," in *2016 IEEE 8th International Conference on Intelligent Systems (IS)*. IEEE, 2016, pp. 646–650.
- [61] Y.-J. Liu, J.-K. Zhang, W.-J. Yan, S.-J. Wang, G. Zhao, and X. Fu, "A main directional mean optical flow feature for spontaneous micro-expression recognition," *IEEE Transactions on Affective Computing*, vol. 7, no. 4, pp. 299–310, 2015.
- [62] L. Lei, J. Li, T. Chen, and S. Li, "A novel graph-tcn with a graph structured representation for micro-expression recognition," in *Proceedings of the 28th ACM International Conference on Multimedia*, 2020, pp. 2237–2245.
- [63] Y. Pei and H. Zha, "3d facial expression editing based on the dynamic graph model," in *2009 IEEE International Conference on Multimedia and Expo*. IEEE, 2009, pp. 1354–1357.
- [64] I. Kotsia and I. Pitas, "Facial expression recognition in image sequences using geometric deformation features and support vector machines," *IEEE transactions on image processing*, vol. 16, no. 1, pp. 172–187, 2006.
- [65] Z. Zhang, T. Wang, and L. Yin, "Region of interest based graph convolution: A heatmap regression approach for action unit detection," in *Proceedings of the 28th ACM International Conference on Multimedia*, 2020, pp. 2890–2898.
- [66] Y. Fan, J. Lam, and V. Li, "Facial action unit intensity estimation via semantic correspondence learning with dynamic graph convolution," in *Proceedings of the AAAI Conference on Artificial Intelligence*, vol. 34, no. 07, 2020, pp. 12 701–12 708.
- [67] Z. Liu, J. Dong, C. Zhang, L. Wang, and J. Dang, "Relation modeling with graph convolutional networks for facial action unit detection," in *International Conference on Multimedia Modeling*. Springer, 2020, pp. 489–501.
- [68] Y.-J. Liu, B.-J. Li, and Y.-K. Lai, "Sparse mdmo: Learning a discriminative feature for spontaneous micro-expression recognition," *IEEE Transactions on Affective Computing*, 2018.
- [69] A. Yao, J. Shao, N. Ma, and Y. Chen, "Capturing au-aware facial features and their latent relations for emotion recognition in the wild," in *Proceedings of the 2015 acm on international conference on multimodal interaction*, 2015, pp. 451–458.
- [70] S. Zafeiriou and I. Pitas, "Discriminant graph structures for facial expression recognition," *IEEE Transactions on Multimedia*, vol. 10, no. 8, pp. 1528–1540, 2008.
- [71] C. Wu, L. Chai, J. Yang, and Y. Sheng, "Facial expression recognition using convolutional neural network on graphs," in *2019 Chinese Control Conference (CCC)*. IEEE, 2019, pp. 7572–7576.
- [72] M. Zhang, Y. Liang, and H. Ma, "Context-aware affective graph reasoning for emotion recognition," in *2019 IEEE International Conference on Multimedia and Expo (ICME)*. IEEE, 2019, pp. 151–156.
- [73] Y. Xie, T. Chen, T. Pu, H. Wu, and L. Lin, "Adversarial graph representation adaptation for cross-domain facial expression recognition," in *Proceedings of the 28th ACM international conference on Multimedia*, 2020, pp. 1255–1264.
- [74] J. Zhou, X. Zhang, Y. Liu, and X. Lan, "Facial expression recognition using spatial-temporal semantic graph network," in *2020 IEEE International Conference on Image Processing (ICIP)*. IEEE, 2020, pp. 1961–1965.
- [75] J. Zhou, X. Zhang, and Y. Liu, "Learning the connectivity: Situational graph convolution network for facial expression recognition," in *2020 IEEE International Conference on Visual Communications and Image Processing (VCIP)*. IEEE, 2020, pp. 230–234.
- [76] H. Chen, Y. Deng, S. Cheng, Y. Wang, D. Jiang, and H. Sahli, "Efficient spatial temporal convolutional features for audiovisual continuous affect recognition," in *Proceedings of the 9th International on Audio/Visual Emotion Challenge and Workshop*, 2019, pp. 19–26.
- [77] A. R. Rivera and O. Chae, "Spatiotemporal directional number transitional graph for dynamic texture recognition," *IEEE transactions on pattern analysis and machine intelligence*, vol. 37, no. 10, pp. 2146–2152, 2015.
- [78] D. Liu, H. Zhang, and P. Zhou, "Video-based facial expression recognition using graph convolutional networks," *arXiv preprint arXiv:2010.13386*, 2020. [Online]. Available: <https://arxiv.org/abs/2010.13386>
- [79] Y. Tong, W. Liao, and Q. Ji, "Facial action unit recognition by exploiting their dynamic and semantic relationships," *IEEE transactions on pattern analysis and machine intelligence*, vol. 29, no. 10, pp. 1683–1699, 2007.
- [80] Y. Zhu, S. Wang, L. Yue, and Q. Ji, "Multiple-facial action unit recognition by shared feature learning and semantic relation modeling," in *2014 22nd International Conference on Pattern Recognition*. IEEE, 2014, pp. 1663–1668.

- [81] L. Lo, H.-X. Xie, H.-H. Shuai, and W.-H. Cheng, "Mer-gcn: Micro-expression recognition based on relation modeling with graph convolutional networks," in *2020 IEEE Conference on Multimedia Information Processing and Retrieval (MIPR)*. IEEE, 2020, pp. 79–84.
- [82] Z. Cui, Y. Zhang, and Q. Ji, "Label error correction and generation through label relationships," in *Proceedings of the AAAI Conference on Artificial Intelligence*, vol. 34, no. 04, 2020, pp. 3693–3700.
- [83] G. Li, X. Zhu, Y. Zeng, Q. Wang, and L. Lin, "Semantic relationships guided representation learning for facial action unit recognition," in *Proceedings of the AAAI Conference on Artificial Intelligence*, vol. 33, no. 01, 2019, pp. 8594–8601.
- [84] C. Corneanu, M. Madadi, and S. Escalera, "Deep structure inference network for facial action unit recognition," in *Proceedings of the European Conference on Computer Vision (ECCV)*, 2018, pp. 298–313.
- [85] H.-X. Xie, L. Lo, H.-H. Shuai, and W.-H. Cheng, "Au-assisted graph attention convolutional network for micro-expression recognition," in *Proceedings of the 28th ACM International Conference on Multimedia*, 2020, pp. 2871–2880.
- [86] K. He, X. Zhang, S. Ren, and J. Sun, "Deep residual learning for image recognition," in *Proceedings of the IEEE conference on computer vision and pattern recognition*, 2016, pp. 770–778.
- [87] L. Zhou, Q. Mao, and M. Dong, "Objective class-based micro-expression recognition through simultaneous action unit detection and feature aggregation," *arXiv preprint arXiv:2012.13148*, 2020. [Online]. Available: <https://arxiv.org/abs/2012.13148>
- [88] R. Walecki, O. Rudovic, V. Pavlovic, B. Schuller, and M. Pantic, "Deep structured learning for facial expression intensity estimation," *Image Vis. Comput.*, vol. 259, pp. 143–154, 2017.
- [89] T. Song, L. Chen, W. Zheng, and Q. Ji, "Uncertain graph neural networks for facial action unit detection," in *Proceedings of the AAAI Conference on Artificial Intelligence*, 2021. [Online]. Available: https://www.researchgate.net/publication/346853340_Uncertain_Graph_Neural_Networks_for_Facial_Action_Unit_Detection
- [90] X. Niu, H. Han, S. Shan, and X. Chen, "Multi-label co-regularization for semi-supervised facial action unit recognition," in *Proceedings of the 33rd Conference on Neural Information Processing Systems*, vol. 32, 2019. [Online]. Available: <https://proceedings.neurips.cc/paper/2019/file/cf67355a3333e6e143439161adc2d82e-Paper.pdf>
- [91] S. Chen, J. Wang, Y. Chen, Z. Shi, X. Geng, and Y. Rui, "Label distribution learning on auxiliary label space graphs for facial expression recognition," in *Proceedings of the IEEE/CVF Conference on Computer Vision and Pattern Recognition*, 2020, pp. 13 984–13 993.
- [92] W.-S. Chien, H.-C. Yang, and C.-C. Lee, "Cross corpus physiological-based emotion recognition using a learnable visual semantic graph convolutional network," in *Proceedings of the 28th ACM International Conference on Multimedia*, 2020, pp. 2999–3006.
- [93] Z. Xu, S. Wang, and C. Wang, "Exploiting multi-emotion relations at feature and label levels for emotion tagging," in *Proceedings of the 28th ACM International Conference on Multimedia*, 2020, pp. 2955–2963.
- [94] W. Zheng, X. Zhou, C. Zou, and L. Zhao, "Facial expression recognition using kernel canonical correlation analysis (kcca)," *IEEE transactions on neural networks*, vol. 17, no. 1, pp. 233–238, 2006.
- [95] D. Derkach and F. M. Sukno, "Local shape spectrum analysis for 3d facial expression recognition," in *2017 12th IEEE International Conference on Automatic Face & Gesture Recognition (FG 2017)*. IEEE, 2017, pp. 41–47.
- [96] H. K. Meena, K. K. Sharma, and S. D. Joshi, "Facial expression recognition using the spectral graph wavelet," *IET Signal Processing*, vol. 13, no. 2, pp. 224–229, 2018.
- [97] R. Zhi, M. Flierl, Q. Ruan, and W. B. Kleijn, "Graph-preserving sparse nonnegative matrix factorization with application to facial expression recognition," *IEEE Transactions on Systems, Man, and Cybernetics, Part B (Cybernetics)*, vol. 41, no. 1, pp. 38–52, 2010.
- [98] H.-W. Kung, Y.-H. Tu, and C.-T. Hsu, "Dual subspace non-negative graph embedding for identity-independent expression recognition," *IEEE Transactions on Information Forensics and Security*, vol. 10, no. 3, pp. 626–639, 2015.
- [99] K. Zhang, Y. Huang, Y. Du, and L. Wang, "Facial expression recognition based on deep evolutionary spatial-temporal networks," *IEEE Transactions on Image Processing*, vol. 26, no. 9, pp. 4193–4203, 2017.
- [100] Y.-H. Oh, J. See, A. C. Le Ngo, R. C.-W. Phan, and V. M. Baskaran, "A survey of automatic facial micro-expression analysis: databases, methods, and challenges," *Frontiers in psychology*, vol. 9, p. 1128, 2018.
- [101] K. Zhao, W.-S. Chu, and H. Zhang, "Deep region and multi-label learning for facial action unit detection," in *Proceedings of the IEEE Conference on Computer Vision and Pattern Recognition*, 2016, pp. 3391–3399.
- [102] V. Kazemi and J. Sullivan, "One millisecond face alignment with an ensemble of regression trees," in *Proceedings of the IEEE conference on computer vision and pattern recognition*, 2014, pp. 1867–1874.
- [103] N. Dalal and B. Triggs, "Histograms of oriented gradients for human detection," in *2005 IEEE computer society conference on computer vision and pattern recognition (CVPR'05)*, vol. 1. Ieee, 2005, pp. 886–893.
- [104] P. Carcagnì, M. Del Coco, M. Leo, and C. Distantè, "Facial expression recognition and histograms of oriented gradients: a comprehensive study," *SpringerPlus*, vol. 4, no. 1, pp. 1–25, 2015.
- [105] D. G. Lowe, "Distinctive image features from scale-invariant keypoints," *International journal of computer vision*, vol. 60, no. 2, pp. 91–110, 2004.
- [106] C. Liu and H. Wechsler, "Independent component analysis of gabor features for face recognition," *IEEE transactions on Neural Networks*, vol. 14, no. 4, pp. 919–928, 2003.
- [107] J. Wang, K. Sun, T. Cheng, B. Jiang, C. Deng, Y. Zhao, D. Liu, Y. Mu, M. Tan, X. Wang et al., "Deep high-resolution representation learning for visual recognition," *IEEE transactions on pattern analysis and machine intelligence*, 2020. [Online]. Available: <https://doi.org/10.1109/TPAMI.2020.2983686>
- [108] B. Xiao, H. Wu, and Y. Wei, "Simple baselines for human pose estimation and tracking," in *Proceedings of the European conference on computer vision (ECCV)*, 2018, pp. 466–481.
- [109] W. Li, F. Abtahi, Z. Zhu, and L. Yin, "Eac-net: A region-based deep enhancing and cropping approach for facial action unit detection," in *2017 12th IEEE International Conference on Automatic Face & Gesture Recognition (FG 2017)*. IEEE, 2017, pp. 103–110.
- [110] G. Zhao and M. Pietikainen, "Dynamic texture recognition using local binary patterns with an application to facial expressions," *IEEE transactions on pattern analysis and machine intelligence*, vol. 29, no. 6, pp. 915–928, 2007.
- [111] M. J. Lyons, J. Budynek, A. Plante, and S. Akamatsu, "Classifying facial attributes using a 2-d gabor wavelet representation and discriminant analysis," in *Proceedings fourth IEEE international conference on automatic face and gesture recognition (Cat. No. PR00580)*. IEEE, 2000, pp. 202–207.
- [112] S. Ren, K. He, R. Girshick, and J. Sun, "Faster r-cnn: towards real-time object detection with region proposal networks," *IEEE transactions on pattern analysis and machine intelligence*, vol. 39, no. 6, pp. 1137–1149, 2016.
- [113] K. Simonyan and A. Zisserman, "Very deep convolutional networks for large-scale image recognition," *arXiv preprint arXiv:1409.1556*, 2014. [Online]. Available: <https://arxiv.org/abs/1409.1556>
- [114] R. A. Kirsch, "Computer determination of the constituent structure of biological images," *Computers and biomedical research*, vol. 4, no. 3, pp. 315–328, 1971.
- [115] D. Tran, H. Wang, L. Torresani, J. Ray, Y. LeCun, and M. Paluri, "A closer look at spatiotemporal convolutions for action recognition," in *Proceedings of the IEEE conference on Computer Vision and Pattern Recognition*, 2018, pp. 6450–6459.
- [116] Y.-I. Tian, T. Kanade, and J. F. Cohn, "Recognizing action units for facial expression analysis," *IEEE Transactions on pattern analysis and machine intelligence*, vol. 23, no. 2, pp. 97–115, 2001.
- [117] Z. Qiu, T. Yao, and T. Mei, "Learning spatio-temporal representation with pseudo-3d residual networks," in *proceedings of the IEEE International Conference on Computer Vision*, 2017, pp. 5533–5541.
- [118] L. Zhou, Q. Mao, and L. Xue, "Dual-inception network for cross-database micro-expression recognition," in *2019 14th IEEE International Conference on Automatic Face & Gesture Recognition (FG 2019)*. IEEE, 2019, pp. 1–5.
- [119] P. Berkes, F. Wood, and J. Pillow, "Characterizing neural dependencies with copula models," in *Advances in neural information processing systems*, vol. 21, 2008, pp. 129–136.
- [120] K. Hara, H. Kataoka, and Y. Satoh, "Can spatiotemporal 3d cnns retrace the history of 2d cnns and imagenet?" in *Proceedings of the*

- IEEE conference on Computer Vision and Pattern Recognition*, 2018, pp. 6546–6555.
- [121] Z. Luo, L. Liu, J. Yin, Y. Li, and Z. Wu, “Deep learning of graphs with ngram convolutional neural networks,” *IEEE Transactions on Knowledge and Data Engineering*, vol. 29, no. 10, pp. 2125–2139, 2017.
- [122] Y. Li and A. Gupta, “Beyond grids: Learning graph representations for visual recognition,” in *Proceedings of the 32nd International Conference on Neural Information Processing Systems*, 2018, pp. 9245–9255.
- [123] C. Kemp and J. B. Tenenbaum, “The discovery of structural form,” *Proceedings of the National Academy of Sciences*, vol. 105, no. 31, pp. 10 687–10 692, 2008.
- [124] S. Bai, J. Z. Kolter, and V. Koltun, “An empirical evaluation of generic convolutional and recurrent networks for sequence modeling,” *arXiv preprint arXiv:1803.01271*, 2018. [Online]. Available: <https://arxiv.org/abs/1803.01271>
- [125] Y. Wang, Y. Sun, Z. Liu, S. E. Sarma, M. M. Bronstein, and J. M. Solomon, “Dynamic graph cnn for learning on point clouds,” *Acm Transactions On Graphics (tog)*, vol. 38, no. 5, pp. 1–12, 2019.
- [126] T. N. Kipf and M. Welling, “Semi-supervised classification with graph convolutional networks,” in *5th International Conference on Learning Representations (ICLR 2017)*, 2017. [Online]. Available: <https://openreview.net/forum?id=SJU4ayYgl>
- [127] T. He and X. Jin, “Image emotion distribution learning with graph convolutional networks,” in *Proceedings of the 2019 on International Conference on Multimedia Retrieval*, 2019, pp. 382–390.
- [128] B. Li, X. Li, Z. Zhang, and F. Wu, “Spatio-temporal graph routing for skeleton-based action recognition,” in *Proceedings of the AAAI Conference on Artificial Intelligence*, vol. 33, no. 01, 2019, pp. 8561–8568.
- [129] M. Defferrard, X. Bresson, and P. Vandergheynst, “Convolutional neural networks on graphs with fast localized spectral filtering,” in *Conference on Neural Information Processing Systems (NeurIPS)*, 2016, pp. 3837–3845.
- [130] P. Veličković, G. Cucurull, A. Casanova, A. Romero, P. Lio, and Y. Bengio, “Graph attention networks,” *arXiv preprint arXiv:1710.10903*, 2017. [Online]. Available: <https://arxiv.org/abs/1710.10903>
- [131] Y. Zhang, S. Pal, M. Coates, and D. Ustebay, “Bayesian graph convolutional neural networks for semi-supervised classification,” in *Proceedings of the AAAI Conference on Artificial Intelligence*, vol. 33, no. 01, 2019, pp. 5829–5836.
- [132] Y. Li, D. Tarlow, M. Brockschmidt, and R. Zemel, “Gated graph sequence neural networks,” in *4th International Conference on Learning Representations (ICLR 2016)*, 2016. [Online]. Available: <https://openreview.net/pdf?id=HJ0NvFzxl>
- [133] G. Zhao, X. Huang, M. Taini, S. Z. Li, and M. Pietikäinen, “Facial expression recognition from near-infrared videos,” *Image and Vision Computing*, vol. 29, no. 9, pp. 607–619, 2011.
- [134] A. Dhall, O. Ramana Murthy, R. Goecke, J. Joshi, and T. Gedeon, “Video and image based emotion recognition challenges in the wild: EmotiW 2015,” in *Proceedings of the 2015 ACM on international conference on multimodal interaction*, 2015, pp. 423–426.
- [135] X. Zhang, L. Yin, J. F. Cohn, S. Canavan, M. Reale, A. Horowitz, P. Liu, and J. M. Girard, “Bp4d-spontaneous: a high-resolution spontaneous 3d dynamic facial expression database,” *Image and Vision Computing*, vol. 32, no. 10, pp. 692–706, 2014.
- [136] W.-J. Yan, X. Li, S.-J. Wang, G. Zhao, Y.-J. Liu, Y.-H. Chen, and X. Fu, “Casme ii: An improved spontaneous micro-expression database and the baseline evaluation,” *PloS one*, vol. 9, no. 1, p. e86041, 2014.
- [137] R. Kosti, J. M. Alvarez, A. Recasens, and A. Lapedriza, “Context based emotion recognition using emotic dataset,” *IEEE transactions on pattern analysis and machine intelligence*, vol. 42, no. 11, pp. 2755–2766, 2019.
- [138] S. M. Mavadati, M. H. Mahoor, K. Bartlett, P. Trinh, and J. F. Cohn, “Disfa: A spontaneous facial action intensity database,” *IEEE Transactions on Affective Computing*, vol. 4, no. 2, pp. 151–160, 2013.
- [139] T. Kanade, J. F. Cohn, and Y. Tian, “Comprehensive database for facial expression analysis,” in *Proceedings Fourth IEEE International Conference on Automatic Face and Gesture Recognition (Cat. No. PR00580)*. IEEE, 2000, pp. 46–53.
- [140] I. J. Goodfellow, D. Erhan, P. L. Carrier, A. Courville, M. Mirza, B. Hamner, W. Cukierski, Y. Tang, D. Thaler, D.-H. Lee *et al.*, “Challenges in representation learning: A report on three machine learning contests,” in *International conference on neural information processing*. Springer, 2013, pp. 117–124.
- [141] A. Dhall, R. Goecke, S. Ghosh, J. Joshi, J. Hoey, and T. Gedeon, “From individual to group-level emotion recognition: EmotiW 5.0,” in *Proceedings of the 19th ACM international conference on multimodal interaction*, 2017, pp. 524–528.
- [142] L. Yin, X. Wei, Y. Sun, J. Wang, and M. J. Rosato, “A 3d facial expression database for facial behavior research,” in *7th international conference on automatic face and gesture recognition (FGRO6)*. IEEE, 2006, pp. 211–216.
- [143] X. Li, T. Pfister, X. Huang, G. Zhao, and M. Pietikäinen, “A spontaneous micro-expression database: Inducement, collection and baseline,” in *2013 10th IEEE International Conference and Workshops on Automatic face and gesture recognition (fg)*. IEEE, 2013, pp. 1–6.
- [144] A. K. Davison, C. Lansley, N. Costen, K. Tan, and M. H. Yap, “Samm: A spontaneous micro-facial movement dataset,” *IEEE transactions on affective computing*, vol. 9, no. 1, pp. 116–129, 2018.
- [145] F. Qu, S.-J. Wang, W.-J. Yan, H. Li, S. Wu, and X. Fu, “Cas(me)²: A database for spontaneous macro-expression and micro-expression spotting and recognition,” *IEEE Transactions on Affective Computing*, vol. 9, no. 4, pp. 424–436, 2018.
- [146] C. Fabian Benitez-Quiroz, R. Srinivasan, and A. M. Martinez, “Emotionet: An accurate, real-time algorithm for the automatic annotation of a million facial expressions in the wild,” in *Proceedings of the IEEE conference on computer vision and pattern recognition*, 2016, pp. 5562–5570.
- [147] Z. Zhang, P. Luo, C. C. Loy, and X. Tang, “From facial expression recognition to interpersonal relation prediction,” *International Journal of Computer Vision*, vol. 126, no. 5, pp. 550–569, 2018.
- [148] S. Li and W. Deng, “Reliable crowdsourcing and deep locality-preserving learning for unconstrained facial expression recognition,” *IEEE Transactions on Image Processing*, vol. 28, no. 1, pp. 356–370, 2019.
- [149] A. Mollahosseini, B. Hasani, and M. H. Mahoor, “Affectnet: A database for facial expression, valence, and arousal computing in the wild,” *IEEE Transactions on Affective Computing*, vol. 10, no. 1, pp. 18–31, 2019.
- [150] M. Valstar and M. Pantic, “Induced disgust, happiness and surprise: an addition to the mmi facial expression database,” in *Proceedings of the 3rd International Workshop on EMOTION (satellite of LREC): Corpora for Research on Emotion and Affect*. Paris, France, 2010, p. 65.
- [151] G. Zhao and X. Li, “Automatic micro-expression analysis: open challenges,” *Frontiers in psychology*, vol. 10, p. 1833, 2019.
- [152] N. Aifanti, C. Papachristou, and A. Delopoulos, “The mug facial expression database,” in *11th International Workshop on Image Analysis for Multimedia Interactive Services WIAMIS 10*. IEEE, 2010, pp. 1–4.
- [153] M. J. Lyons, J. Budynek, and S. Akamatsu, “Automatic classification of single facial images,” *IEEE transactions on pattern analysis and machine intelligence*, vol. 21, no. 12, pp. 1357–1362, 1999.
- [154] R. Zhi, M. Liu, and D. Zhang, “A comprehensive survey on automatic facial action unit analysis,” *The Visual Computer*, vol. 36, no. 5, pp. 1067–1093, 2020.
- [155] W.-J. Yan, Q. Wu, Y.-J. Liu, S.-J. Wang, and X. Fu, “Casme database: a dataset of spontaneous micro-expressions collected from neutralized faces,” in *2013 10th IEEE international conference and workshops on automatic face and gesture recognition (FG)*. IEEE, 2013, pp. 1–7.
- [156] E. A. Haggard and K. S. Isaacs, “Micromomentary facial expressions as indicators of ego mechanisms in psychotherapy,” in *Methods of research in psychotherapy*. Springer, 1966, pp. 154–165.
- [157] P. Ekman and W. V. Friesen, “Nonverbal leakage and clues to deception,” *Psychiatry*, vol. 32, no. 1, pp. 88–106, 1969.
- [158] P. Lucey, J. F. Cohn, K. M. Prkachin, P. E. Solomon, and I. Matthews, “Painful data: The unbc-mcmaster shoulder pain expression archive database,” in *2011 IEEE International Conference on Automatic Face & Gesture Recognition (FG)*. IEEE, 2011, pp. 57–64.
- [159] J. A. M. Correa, M. K. Abadi, N. Sebe, and I. Patras, “Amigos: A dataset for affect, personality and mood research on individuals and groups,” *IEEE Transactions on Affective Computing*, 2018.
- [160] R. Subramanian, J. Wache, M. K. Abadi, R. L. Vieriu, S. Winkler, and N. Sebe, “Ascertain: Emotion and personality recognition using commercial sensors,” *IEEE Transactions on Affective Computing*, vol. 9, no. 2, pp. 147–160, 2016.

- [161] S. Wang, Z. Liu, S. Lv, Y. Lv, G. Wu, P. Peng, F. Chen, and X. Wang, "A natural visible and infrared facial expression database for expression recognition and emotion inference," *IEEE Transactions on Multimedia*, vol. 12, no. 7, pp. 682–691, 2010.
- [162] A. Schaefer, F. Nils, X. Sanchez, and P. Philippot, "Assessing the effectiveness of a large database of emotion-eliciting films: A new tool for emotion researchers," *Cognition and emotion*, vol. 24, no. 7, pp. 1153–1172, 2010.
- [163] M. Behzad, N. Vo, X. Li, and G. Zhao, "Landmarks-assisted collaborative deep framework for automatic 4d facial expression recognition," in *2020 15th IEEE International Conference on Automatic Face and Gesture Recognition (FG 2020)*. IEEE, 2020, pp. 1–5.
- [164] D. Kollias and S. Zafeiriou, "Expression, affect, action unit recognition: Aff-wild2, multi-task learning and arcface," *arXiv preprint arXiv:1910.04855*, 2019. [Online]. Available: <https://arxiv.org/abs/1910.04855>
- [165] D. Kollias, A. Schulc, E. Hajiyeve, and S. Zafeiriou, "Analysing affective behavior in the first abaw 2020 competition," in *2020 15th IEEE International Conference on Automatic Face and Gesture Recognition (FG 2020)*. IEEE Computer Society, 2020, pp. 794–800.
- [166] X. Huang, A. Dhall, R. Goecke, M. Pietikäinen, and G. Zhao, "Multimodal framework for analyzing the affect of a group of people," *IEEE Transactions on Multimedia*, vol. 20, no. 10, pp. 2706–2721, 2018.